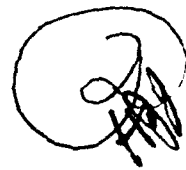


AD-A267 967



AUTOMATED SHIRT  
COLLAR MANUFACTURING

DLA 900-87-0017 Task 0014

FINAL REPORT

VOLUME II:

Collar Band Folding and Fixing

**S** DTIC  
ELECTE  
AUG 04 1993  
**A** **D**

Marvin W. Dixon  
Principal Investigator

and

Joseph Benjamin Long  
Research Assistant

This document has been approved  
for public release and sale; its  
distribution is unlimited.

Center for Advanced Manufacturing  
and  
Clemson Apparel Research

Clemson University  
Clemson, SC

June 1992

93-17368



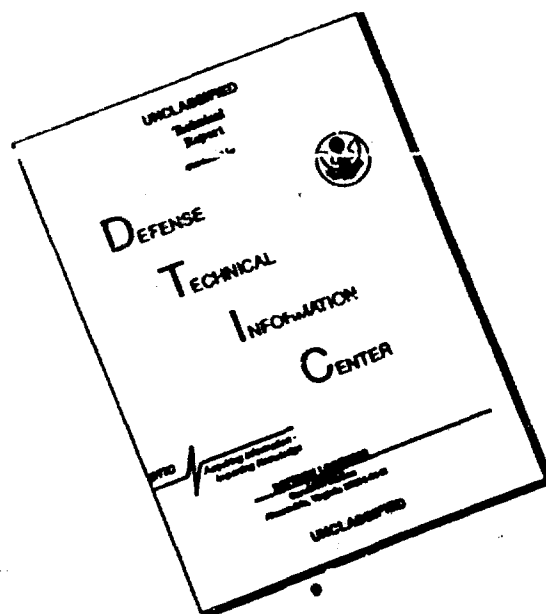
131P8

93 8 3 060

## REPORT DOCUMENTATION PAGE

1a. REPORT SECURITY CLASSIFICATION Unclassified			1b. RESTRICTIVE MARKINGS	
2a. SECURITY CLASSIFICATION AUTHORITY			3. DISTRIBUTION/AVAILABILITY OF REPORT Unclassified Distribution Unlimited	
2b. DECLASSIFICATION/DOWNGRADING SCHEDULE			5. MONITORING ORGANIZATION REPORT NUMBER(S)	
1. PERFORMING ORGANIZATION REPORT NUMBER(S)			7a. NAME OF MONITORING ORGANIZATION Defense Personnel Support Center	
5a. NAME OF PERFORMING ORGANIZATION Clemson University/ Clemson Apparel Research		6b. OFFICE SYMBOL (If applicable)	7b. ADDRESS (City, State, and ZIP Code) 2800 South 20th Street P.O. Box 8419 Philadelphia, PA 19101-8419	
5c. ADDRESS (City, State, and ZIP Code) 500 Lebanon Road Pendleton, SC 29670		8b. OFFICE SYMBOL (If applicable)	9. PROCUREMENT INSTRUMENT IDENTIFICATION NUMBER DLA 900-87-D-0017 Delivery Order 0014	
5a. NAME OF FUNDING/SPONSORING ORGANIZATION Defense Logistics Agency		8b. OFFICE SYMBOL (If applicable)	10. SOURCE OF FUNDING NUMBERS	
5c. ADDRESS (City, State, and ZIP Code) Room 4B195 Cameron Station Alexandria, VA 22304-6100		PROGRAM ELEMENT NO. 78011S	PROJECT NO.	TASK NO.
		WORK UNIT ACCESSION NO.		
1. TITLE (Include Security Classification) Automated Shirt Collar Manufacturing Vol. II: Collar Band Folding and Fixing - unclassified				
12. PERSONAL AUTHOR(S) M. W. Dixon, Principal Investigator; Joseph Benjamin Long, Research Assistant				
13a. TYPE OF REPORT Final		13b. TIME COVERED FROM n/a TO	14. DATE OF REPORT (Year, Month, Day) 1992 June 23	15. PAGE COUNT 121
16. SUPPLEMENTARY NOTATION				
17. COSATI CODES			18. SUBJECT TERMS (Continue on reverse if necessary and identify by block number)	
FIELD	GROUP	SUB-GROUP		
19. ABSTRACT (Continue on reverse if necessary and identify by block number) This document presents Volume II of the report of research into automated shirt collar manufacturing which address collar band folding and fixing. Specifically presented in this volume is the result of research into the folding and fixing of woven fabrics, so that banded shirt collars might be automatically manufactured, without the use of adhesives. This was accomplished by folding collar bands through the use of moisture, heating, and cooling. The use of conductive heating and cooling was found to be especially effective in tests conducted on two proof-of-concept machines developed by JetSew and Clemson University.				
20. DISTRIBUTION/AVAILABILITY OF ABSTRACT <input checked="" type="checkbox"/> UNCLASSIFIED/UNLIMITED <input type="checkbox"/> SAME AS RPT. <input type="checkbox"/> OTC USERS			21. ABSTRACT SECURITY CLASSIFICATION Unclassified	
22a. NAME OF RESPONSIBLE INDIVIDUAL Frank W. Paul			22b. TELEPHONE (Include Area Code) 303-656-3291	22c. OFFICE SYMBOL

# DISCLAIMER NOTICE



THIS DOCUMENT IS BEST QUALITY AVAILABLE. THE COPY FURNISHED TO DTIC CONTAINED A SIGNIFICANT NUMBER OF PAGES WHICH DO NOT REPRODUCE LEGIBLY.

# ACKNOWLEDGMENTS

The authors would like to thank all those who were involved with support of this project. Especially, it is appropriate to thank the Defense Logistics Agency, Department of Defense, for support of this work under contract number DLA 900-87-0017 Task 0014. This work was conducted through Clemson Apparel Research, a facility whose purpose is the advancement of apparel manufacturing technology, by the Center for Advanced Manufacturing, Clemson University and Jet Sew, Barneveld, N.Y.

Accession For	
NTIS CRA&I	<input checked="" type="checkbox"/>
DTIC TAB	<input type="checkbox"/>
Unannounced	<input type="checkbox"/>
Justification	
By	
Distribution/	
Availability Codes	
Dist	Avail. and/or Special
A-1	

DTIC QUALITY INSPECTED 3

## ABSTRACT

The focus of this research was the folding and fixing of woven fabrics with direct applicability to automating the manufacture of banded-collared shirts. The objective of this research was to establish a process by which woven fabrics consisting of either 100% cotton, 100% polyester, or cotton/polyester blends could be folded without the use of adhesives.

A test fixture was designed and built to establish physical parameters required for folding and fixing woven fabrics, namely temperature, moisture, and pressure. Quantitative results from the experimental program were used to establish design criteria by which two operational folding mechanisms were designed and fabricated. Each mechanism employed a different process for folding and creasing the fabric.

The first device employed superheated steam for wetting, heating, and drying the fabric. A portable steam generator was utilized for producing saturated steam. An in-line tube superheater with a variable power source was used to heat the steam to the desired temperature. A steam manifold with a sintered bronze top plate was used as the folding bed assembly, allowing the superheated steam to directly pass through the fabric sample.

The second device employed conductive heating and cooling for heating and cooling the fabric. The folding operation was conducted at five sequential stations in the mechanism

where loading, folding, heating, cooling, and unloading occurred. Heating was provided by cartridge heaters in blocks of aluminum. Cooling was provided by vortex coolers with air channels machined inside blocks of aluminum. Moisture was added manually prior to loading in cases containing high cotton content.

The two mechanisms were evaluated based on fold performance and cycle time. Fold performance was determined based upon fold characteristics measured with the use of an overhead projector and a hand caliper or machinist's scale. Cycle times were tabulated for each type of fabric. The superheated steam technique was faster for fabrics containing a high content of cotton, whereas conductive heating and cooling was faster for folding fabrics containing a high content of polyester. The highest cycle time recorded for the superheated steam device was 56 seconds in the case of the 70/30 polyester/cotton blend. The lowest cycle time was recorded as 22 seconds in the case of 100% cotton. The cycle times of the conductive heating and cooling device ranged from 15 seconds in the case of 100% polyester to 80 seconds in the case of 100% cotton.

Since both mechanisms performed comparably on 100% polyester, and since the conductive heating and cooling device operated at markedly higher cycle times on the high cotton content fabrics, the author suggests that further research include refining the superheated steam process to determine whether or not it can be made more efficient with respect to high polyester content materials.

## TABLE OF CONTENTS

	Page
TITLE PAGE .....	i
ABSTRACT .....	ii
LIST OF TABLES .....	vi
LIST OF FIGURES .....	vii
 CHAPTER	
I.    INTRODUCTION .....	1
Statement of Need .....	1
Overview of Preliminary Laboratory Experimentation .....	6
Design Objective .....	7
Overview of Design Tasks .....	8
II.   DEFINING CREASING PROCEDURE AND PARAMETERS .....	10
Introduction .....	10
Test Fixture .....	10
Quantification of Parameters and Preliminary Results .....	12
The Design Criteria .....	17
III.  PRESENTATION OF TWO ALTERNATIVE PROOF- OF-CONCEPT DEVICES .....	19
Introduction .....	19
Clemson Design .....	20
Jet Sew Design .....	30
IV.   EXPERIMENTAL SETUP AND METHODOLOGY .....	37
Introduction .....	37
Fold Evaluation .....	38
Experimental Methods .....	44
Discussion of Results .....	49
Comparison of Results .....	53

## Table of Contents (Continued)

	Page
V. CONCLUSIONS AND RECOMMENDATIONS .....	57
Introduction .....	57
Conclusions .....	58
Recommendations .....	59
APPENDICES .....	61
A. Tabulated Safe Ironing Temperatures .....	62
B. Generation of Alternatives .....	63
C. Heat Transfer Analysis - Implicit Finite-Difference Model .....	75
D. Program Listings for Implicit Finite- Difference Model of Porous Materials and Steel Folding Blades .....	79
E. Output from Finite-Difference Models .....	86
F. System Thermodynamic Considerations for Clemson Device .....	93
G. Error Factors in Temperature Readings .....	96
H. Uncertainty Analysis in Measured Quantities .....	101
I. Tabulated Experimental Results - Clemson Device .....	104
J. Tabulated Experimental Results - Jet Sew Device .....	115
LIST OF REFERENCES .....	121



## LIST OF FIGURES

Figure	Page
1. Shirt Collar Configurations .....	2
2. Collar Band Assembly .....	3
3. Proper Edge Fold in Cross-section .....	5
4. Test Fixture .....	11
5. Test Fixture Configurations .....	13
6. Test Fixture Folding Operation .....	14
7. Clemson Folding Unit .....	22
8. Clemson Folding Operation .....	24
9. Clemson System Layout .....	28
10. Schematic of Jet Sew System Layout Indicating Five Sequential Operating Stations .....	31
11. Jet Sew Folding Unit .....	32
12. Jet Sew Folding Operation .....	33
13. Fold Characteristics .....	39
14. Cross-Sections of Actual Folds as Seen under Microscope .....	42
B-1. Alternative 1. Cross-section of Folding Cavity .....	64
B-2. Alternative 1. 8 Steps of Operation with Heating and Cooling through Blades .....	65
B-3. Alternative 2. Cross-section of Folding Cavity .....	67
B-4. Alternative 2. 8 Steps of Operation with Heating and Cooling through Thin Membrane .....	68
B-5. Alternative 3. Cross-section of Folding Cavity .....	70

## LIST OF TABLES

Table	Page
I. Design Parameters for a Successful Crease .....	17
II. Limiting Values of Folding Parameters for Clemson Device .....	54
III. Limiting Values of Folding Parameters for Jet Sew Device .....	55
H-I. Uncertainties in Measured Quantities .....	102

## List of Figures (Continued)

Figure	Page
B-6. Alternative 3. 8 Steps of Operation with Multi-stage Folding Cavity Using Heating and Cooling Stations .....	71
B-7. Alternative 4. Cross-section of Folding Cavity .....	73
B-8. Alternative 4. 8 Steps of Operation with Modified Mandiel Design .....	74
C-1. Cross-section of Porous Material Indicating Elemental Discretization and Boundary Conditions .....	76
G-1. Thermocouple Approximation .....	97
G-2. System Parameters - Fin Approximation .....	99
I-1. Moisture Content vs. Time for 70/30 Poly/Cotton Blend .....	111
I-2. Moisture Content vs. Time for 55/45 Poly/Cotton Blend .....	112
I-3. Moisture Content vs. Time for 65/35 Cotton/Poly Blend .....	113
I-4. Moisture Content vs. Time for 100% Cotton Fabric .....	114

## CHAPTER I

### INTRODUCTION

#### Statement of Need

At present, there are two basic types of collars which are used on men's shirts. One type, which might be referred to as a "sport collar," is sewn directly to the body of the shirt. The "sport collar" lies flat on the shirt body when worn, and normally is not used when wearing a necktie.

"Dress collars," the second basic type of collar, incorporate a "collar band" which is sewn between the collar and the shirt body. A "dress collar," also called a "banded shirt collar", does not lie flat on the shirt body, but allows space between the collar and the shirt body for a necktie (see Figure 1).

A collar band consists of two identical pieces of fabric, an inner face and an outer face, which are contoured to match the shape of the collar on one edge and the shape of the shirt body on the other edge. A collar band is normally about 1 1/2 inches wide, and is the length of the neck size of the shirt. The collar is placed between the inner and outer faces on one edge of the band, and the shirt body is placed between the inner and outer faces on the other edge of the band. Each edge of the collar band is sewn to fix the collar to the shirt body (see Figure 2).

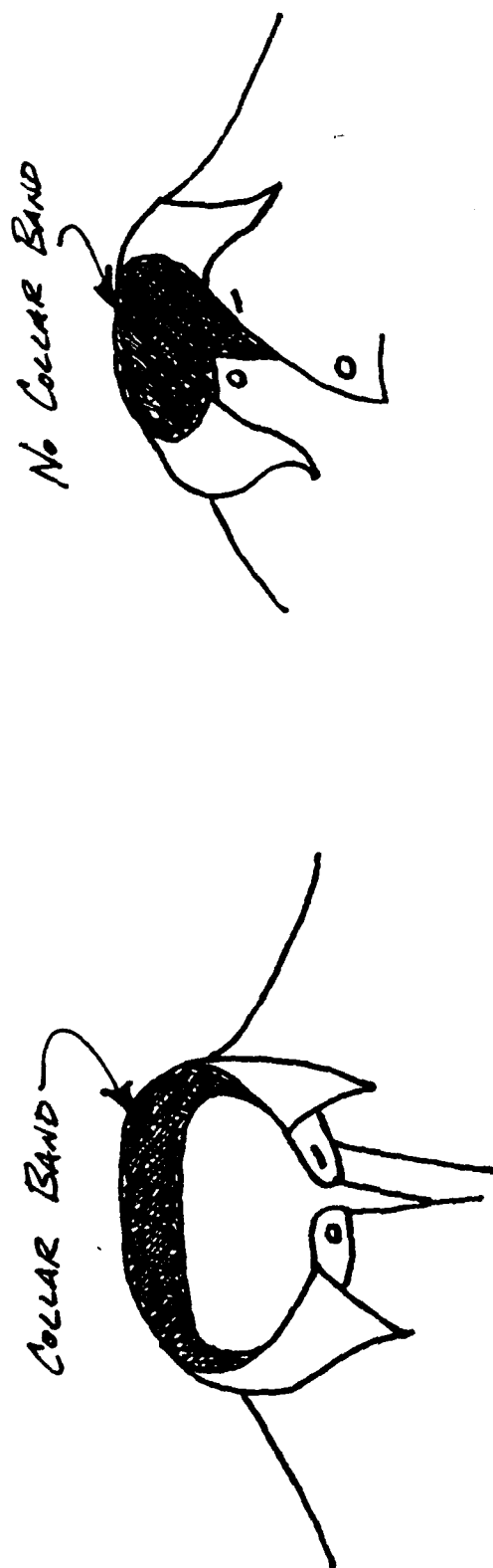


Figure 1. Collar Configurations

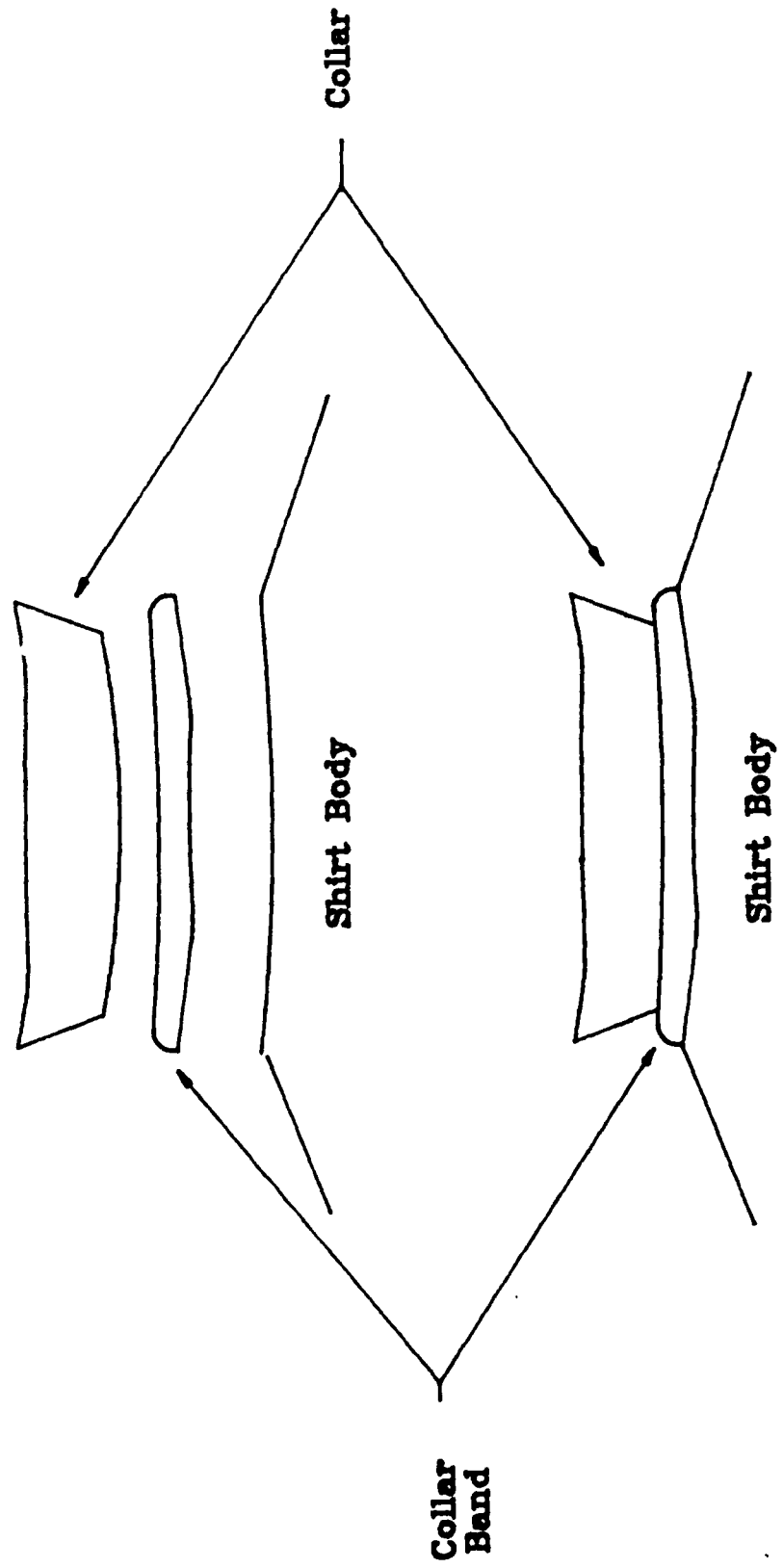


Figure 2. Collar Band Assembly

Prior to sewing the collar band to the collar and the shirt body, each edge of the contoured inner or outer face is folded to eliminate exposure of any frayed fabric edges. The fold, which is normally made with approximately 1/4 inch of material and is confined to the edges of the collar band, is called an "edge fold". The result is a single ply of material with an edge fold around its perimeter which has the same contoured shape as the original flat piece of fabric. Two of these single plies with edge folds, an outer and an inner face, are sewn together with the collar on one edge and the shirt body on the other edge to form a "banded shirt collar" (refer again to Figure 2).

Automation practices in today's apparel industry require an edge fold in collar bands. Collar bands are made and stored separately from the collar and the shirt body, so a folded inner or outer face of a collar band may be held for several minutes or even several days before being sewn to the collar and the shirt body. Hence, an edge fold on an outer or inner face of a collar band must remain until it is used during shirt assembly.

Not only must an edge fold remain for an indefinite period of time, but the fold must also be relatively flat to insure that the fabric can be sewn along the edge. In other words, the folded edge must lie close to the body of the inner or outer face and must not "stand up" (see Figure 3). Therefore, a successful fold must be relatively flat over long periods of time.

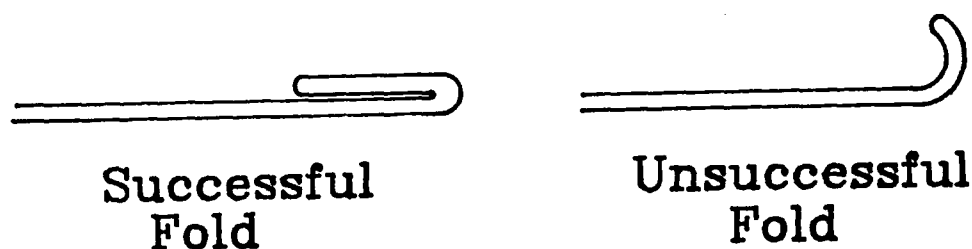


Figure 3. Proper Edge Fold in Cross-section

In order to achieve a successful fold, a layer of fabric impregnated with an adhesive is used currently to aid in edge folding and to maintain the crease. This adhesive layer, called an "interliner," essentially glues the edge fold to the body of the collar band when the interliner is heated by a hot surface.

The adhesive interliner helps to maintain a flat fold over long periods of time, but this additional layer of fabric increases the cost of the shirt and produces a bulky collar band. By adding one adhesive interliner to each face of a collar band, two additional layers of material are added to each collar assembly. Then, in turn, when the edge folds are made, the result is essentially four additional plies of fabric added to each edge where the collar band is sewn. Thus, a process which will allow the folding and fixing of collar



bands without the use of these "adhesive interliners" will decrease product cost and increase product quality.

The objective of this research was to design and fabricate a proof-of-concept apparatus for creating successful folds in woven fabrics without the use of adhesive interliners. The apparatus was used to illustrate the folding process and to quantify process parameters which could be used in the design of second generation prototypes.

#### Overview of Preliminary Laboratory Experimentation

Since the objective of the research addressed folding fabrics for use in automated shirt manufacture, the fabrics tested were limited to 100% cotton, 100% polyester, and cotton/polyester blends, which are the primary materials currently used in the manufacture of shirts.

In order to create a successful fold without the use of an adhesive interliner, it was necessary to establish a parameter set and a folding procedure for folding woven fabrics. A literary search revealed no comprehensive data listing a complete set of folding parameters or parameter ranges. The only information found was presented in Apparel Manufacturing Handbook[1] for safe ironing temperatures. This information is completely displayed in Appendix A.

Since needed information was unavailable, a test fixture was designed and built to determine the physical parameters required to achieve successful folds in woven fabrics. .

Experimentation with various cotton/polyester blend fabrics established the parameter set and the parameter ranges needed for folding. Moisture is needed to relax cotton fibers to allow creasing, then heat is needed for moisture retraction. Retracting moisture from the cotton fibers while folded ensures that the fibers maintain their shape, thus creating the fold. Polyester fibers need to be heated above their heat-set temperature and then cooled for the fibers to maintain the crease. No moisture is necessary in folding polyester fabrics. Various blends of cotton and polyester require different amounts of heating, cooling, and moisture addition and retraction for adequate folding.

Fold characteristics also vary with sizing or other additives placed on the fabric during processing. As a result, pressure is required during heating, moisture addition and retraction, and cooling to fold some types of fabric. These parameter ranges have been quantified and are presented in this thesis.

#### Design Objective

The objectives of this thesis were to: (1) develop and refine temperature, moisture, pressure, and time relationships which are required for folding woven fabrics, (2) to design and build a test apparatus to illustrate the folding process, and (3) to provide a comparison between two possible designs used to fold woven fabrics.

### Overview of Design Tasks

Since a literature search did not yield adequate information regarding folding parameters and folding techniques, a fully operational test fixture was designed and fabricated to determine which physical parameters governed folding of woven fabrics and to establish gross ranges for these parameter values which could be used to develop design criteria for the development of a proof-of-concept apparatus. The test fixture is presented in Chapter II, along with the presentation of the design criteria.

Having established a working set of design criteria, the proof-of-concept folding mechanism was designed so as to provide those physical parameters identified as required for folding woven fabrics. The use of superheated steam was implemented into the design to provide heating, wetting, and drying of the materials. To the author's knowledge, superheated steam has not been used in such a manner. In conjunction with the Mechanical Engineering Department of Clemson University, Jet Sew, of Barneveld, New York, developed an alternative proof-of-concept mechanism which was used to establish a second method of folding woven fabric samples. The layout and operation of each machine, along with information regarding the actual design of the Clemson device, are presented in Chapter III.

Both the Clemson mechanism and the Jet Sew mechanisms were operated and evaluated at Clemson University. Both mechanisms were evaluated using the same criteria for a

THIS  
PAGE  
IS  
MISSING  
IN  
ORIGINAL  
DOCUMENT

## CHAPTER II

### DEFINING CREASING PROCEDURE AND CREASING PARAMETERS

#### Introduction

A test fixture was designed and built for two primary reasons. First, the test fixture demonstrated that woven fabrics could be folded without the use of adhesive interliners. Second, the test fixture was used to determine those physical parameters which governed fabric creasing and gross limits and ranges of those parameters. The data which was obtained from the operation of the test fixture was largely qualitative. However, some quantitative ranges were established through the use of the test fixture which were used as guidelines in developing criteria for the design of the proof-of-concept apparatus.

#### Test Fixture

The test fixture is shown in Figure 4. The fixture consisted of a folding blade, a pressing block, a pressing bed, and a pressing cavity. The pressing block was attached to the base of a household iron (not shown) for heating. The pressing bed was attached to a base and rested in the pressing cavity. The pressing cavity was cut out of a plate that moved vertically. When the plate was in its uppermost position, the top surface of the pressing bed lay approximately 1/8 inch below the top surface of the plate. When

the plate was in its lowest position, the pressing bed filled the entire cavity and protruded above the surface of the plate. These configurations are shown in Figure 5. Pneumatic cylinders actuated the plate in the vertical direction.

The selected method of folding is shown in Figure 6. In the first step of the folding operation, the test sample was placed over the cavity. The folding blade was then placed on top of the sample in the cavity. In this configuration, the folding blade rested on the test sample which rested on the pressing bed. Because the test sample was forced into a smaller cavity, its edges were folded upward. At this point, in step 3, the pressing block slid to the sample and folded the edges flat against the sample. In step 4, the folding blade was removed. The pneumatic cylinders were then discharged, allowing the pressing block (via the iron) to apply heat and pressure to the sample.

#### Quantification of Parameters and Preliminary Results

Different weaves, finishes, and thicknesses of fabric of content 100% cotton were folded using the test fixture. Also tested were fabrics consisting of 50% polyester and 50% cotton, as well as 100% polyester. Each fabric was tested at pressing block temperatures ranging from 325 to 410°F using four different test conditions: (1) heated dry and air cooled; (2) heated dry and conduction cooled (i.e., cooling block); (3) heated damp fabric and air cooled; and (4) heated damp fabric and conduction cooled.

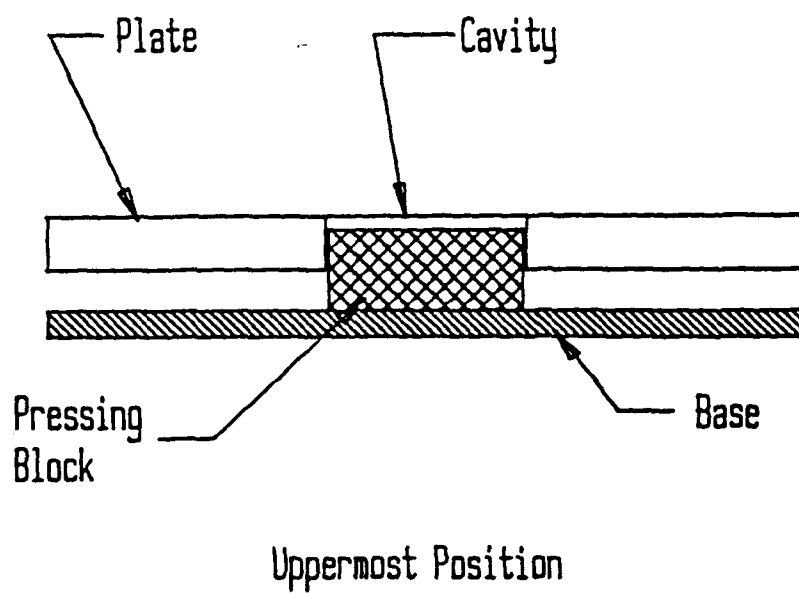


Figure 5. Test Fixture Configuration

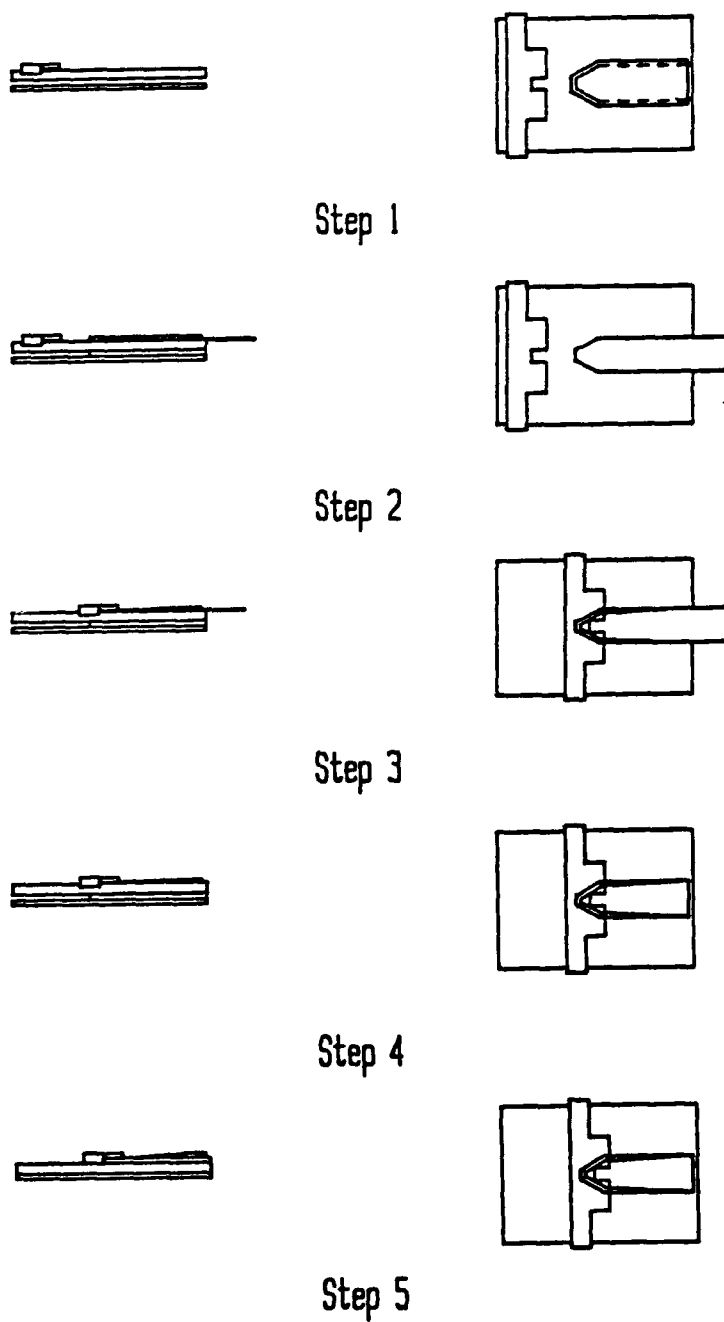


Figure 6. Test Fixture Folding Operation



### 100% Cotton Fabrics

The 100% cotton fabrics showed a permanent crease characterized by no springback when pressed damp at 400° and either air cooled or cooled with the cooling block. The cotton fabrics could not be folded without the addition of moisture to relax the fibers. Heating the fabric evaporated the moisture. It was the retraction of moisture that forced the cotton fibers to maintain the crease.

### 50/50 Cotton/Polyester Blends

Each of the four basic tests described above were performed on 50/50 cotton/polyester blends at a temperature range of 360-370°. Once again, the addition of water was required for permanent creasing. Without water, the material showed a definite crease, but exhibited unacceptable springback over time. To maintain the fold, the fabric must be cooled in the fixture but using the cooling block did not increase the folding performance significantly over air cooling. Therefore, the 50/50 cotton/ polyester blend needed both moisture addition and retraction, as well as heating and cooling to create a successful fold.

### 100% Polyester

At temperatures greater than 375°F, 100% polyester materials became damaged. The fabric became mis-shaped and also discolored from prolonged heat contact. Moisture

addition did not affect the crease characteristics, but fabric cooling while the cloth was held in place allowed the cloth to maintain its creased configuration. Crease characteristics did not appear to change whether the fabric was air cooled or cooled by block. However, cooling was necessary for the fabric to maintain a crease. Polyester fabric must be heated above its thermal set temperature to relax the fibers and then cooled below the thermal set temperature for the fabric to maintain a crease.

#### Summary

Table I summarizes the conclusions drawn from the data obtained by using the test fixture. The table lists those physical parameters which were identified as integral to the folding process, i.e., moisture addition and retraction, heating, cooling, and application of pressure.

Table I. Design Parameters for a Successful Crease

Material	Moisture Addition	Heating Temp (F)	Pressure
100% Cotton	yes	400	no
100% Cotton Crease Resistant	yes	400-410	yes
50/50 Cotton/Polyester	yes	360-370	no
100% Polyester	no	350-375	no

Test fabrics included different weaves, prints, and thicknesses of 100% cotton, 50/50 polyester/cotton blends, and 100% polyester. Since the addition of water improved the crease characteristics for both the 100% cotton and the 50/50 blends, it appeared that the cotton threads required moisture to relax the cotton fibers. In fact, it was the retraction of water from the cotton fibers that created a permanent crease. Contrarily, the polyester fabric reacted as any heat set polymer is expected. Heat relaxed the polymer fibers while cooling set the fabric in the desired position.

#### The Design Criteria

Using the data obtained from the test fixture as a guideline, quantitative ranges were established which were used in developing a proof-of-concept apparatus. The

apparatus needed to provide control of moisture content, temperature, and pressure were variables. The ranges for the creasing parameters were, therefore, the criteria by which the machine was built, tested, and evaluated. The quantified design parameters were:

moisture content: 0 - 20% by fabric sample mass

temperature: 300 - 425°F

folding pressure: 0 - 40 psi.

In summary, a test fixture was designed, built, and operated in order to determine which physical parameters were required to fold woven fabrics. The test fixture was also used to establish gross, quantified ranges of each of these physical parameters. The gross ranges were then used to derive the design criteria for the actual proof-of-concept device. Chapter III will discuss in detail each of two proof-of-concept devices, one developed at Clemson University in Clemson, South Carolina, and one developed at Jet Sew of Barneveld, New York.

CHAPTER III  
PRESENTATION OF TWO ALTERNATIVE  
PROOF-OF-CONCEPT DEVICES

Introduction

This research project was a combined effort of Jet Sew in Barneveld, NY, and of Clemson University, in Clemson, SC, under the direction of the Defense Logistics Agency. To reiterate the purpose of the research, the objectives for designing and building a folding apparatus were: (1) to develop and refine temperature, moisture, pressure, and time relationships which are required for folding woven fabrics, and (2) to illustrate the folding process.

Once the design criteria were set using the quantitative ranges for each folding parameter established with the test fixture, alternative solutions were generated for the configuration of the folding apparatus. The alternatives were generated using a morphological approach, in which the design problem was broken into several different parts. Each part was addressed separately with the intent of generating the largest number of alternatives from which the best one would be selected as the final design. Means of adding and retracting moisture, heating and cooling, and pressure application were investigated separately. Different processes for mechanically folding the fabric were also investigated.

There were two basic categories by which heat transfer could be classified in each mechanism. The mechanisms fell into the following two categories based on the method of heat transfer used: (1) those mechanisms which used conductive heating and cooling, and (2) those mechanisms which used convective heating and cooling. Jet Sew developed a mechanism which utilized conduction, and Clemson University developed a machine which utilized convection. Several alternatives, each utilizing different means of moisture addition and retraction, heating and cooling, and pressure application, were generated in the development of the Clemson device. Each of these alternatives is discussed in detail in Appendix B.

This chapter presents the two alternatives which were developed into working prototypes, i.e., the Clemson design and the Jet Sew design. The principles of operation of each mechanism are explained along with a detailed presentation of each system layout and the operating procedures employed with each mechanism.

#### Clemson Design

Congruant to using convective heating and cooling to fold woven fabrics, Clemson University pursued the application of superheated steam to potentially provide heating, moisture addition and moisture retraction. Superheated steam drying is a process currently used in industries such as grain storage and timber processing for moisture content control.

If there is an influx of superheated steam onto a surface which is at a steady state temperature less than the saturation temperature of the steam, moisture may condense from the steam until the energy from the steam heats the surface to the steam saturation temperature. Then, as the superheated steam continues to flow and the surface is heated, the condensate would evaporate while the surface continues to be heated above that of the saturation temperature of the steam.

Applying these ideas to the folding mechanism, it is conceivable that an influx of steam onto a folding mechanism, with folding mechanism temperature below the steam saturation point would cause condensation, thus providing moisture for wetting the fabric. As steam continues to flow it would heat the fabric and the folding mechanism above the saturation temperature and evaporates the condensed moisture from the fabric.

#### Folding Unit Layout and Operation

A folding apparatus was designed and built for the purpose of utilizing the superheated steam concept. The folding mechanism consisted of four basic parts, as shown in Figure 7: the stationary top plate, the pneumatically actuated folding blades, the pneumatically actuated pressing bed assembly, and the folding mandrel (not pictured). The pressing bed assembly was composed of the steam manifold and the sintered bronze pressing plate. The steam manifold had

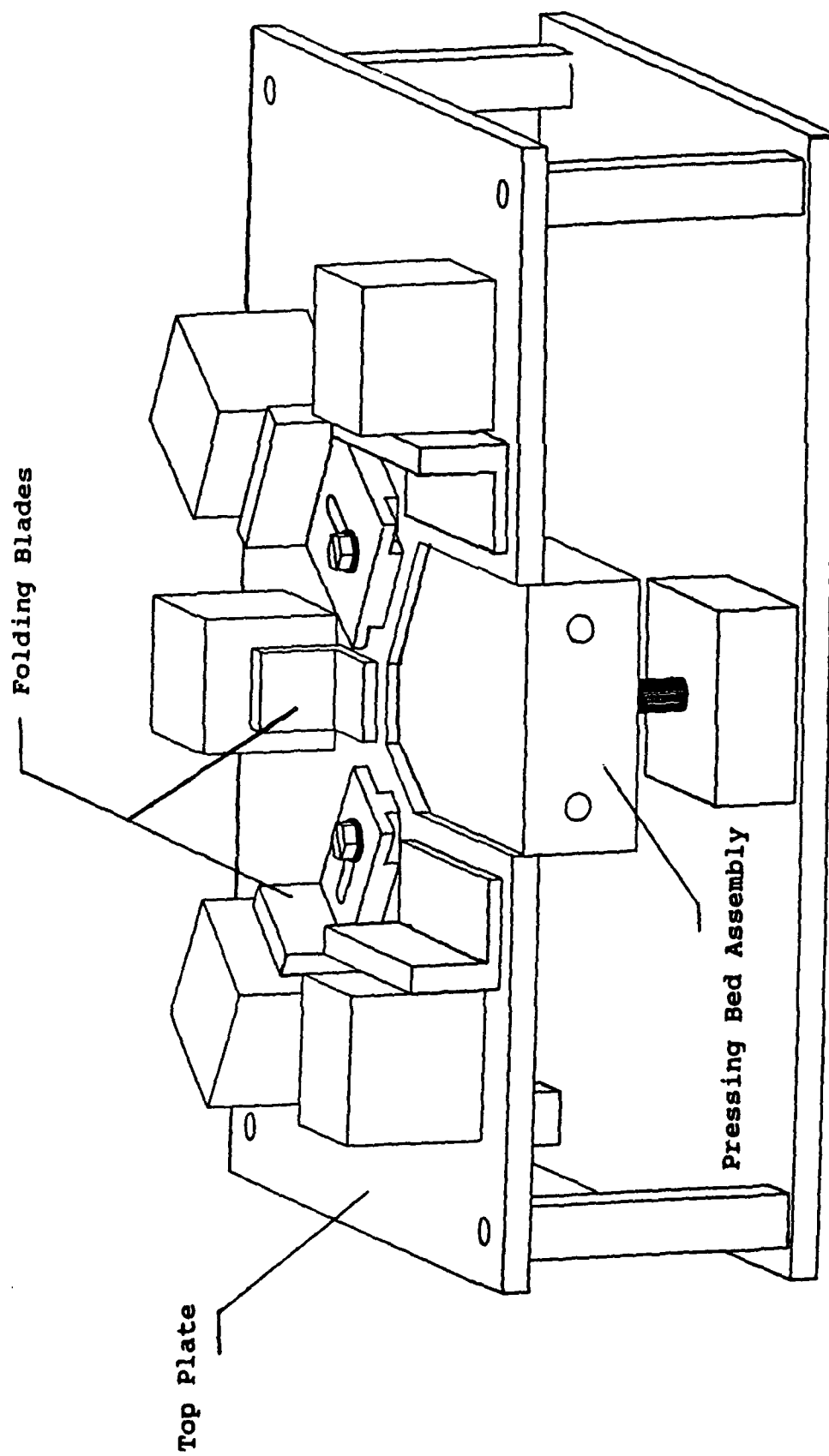
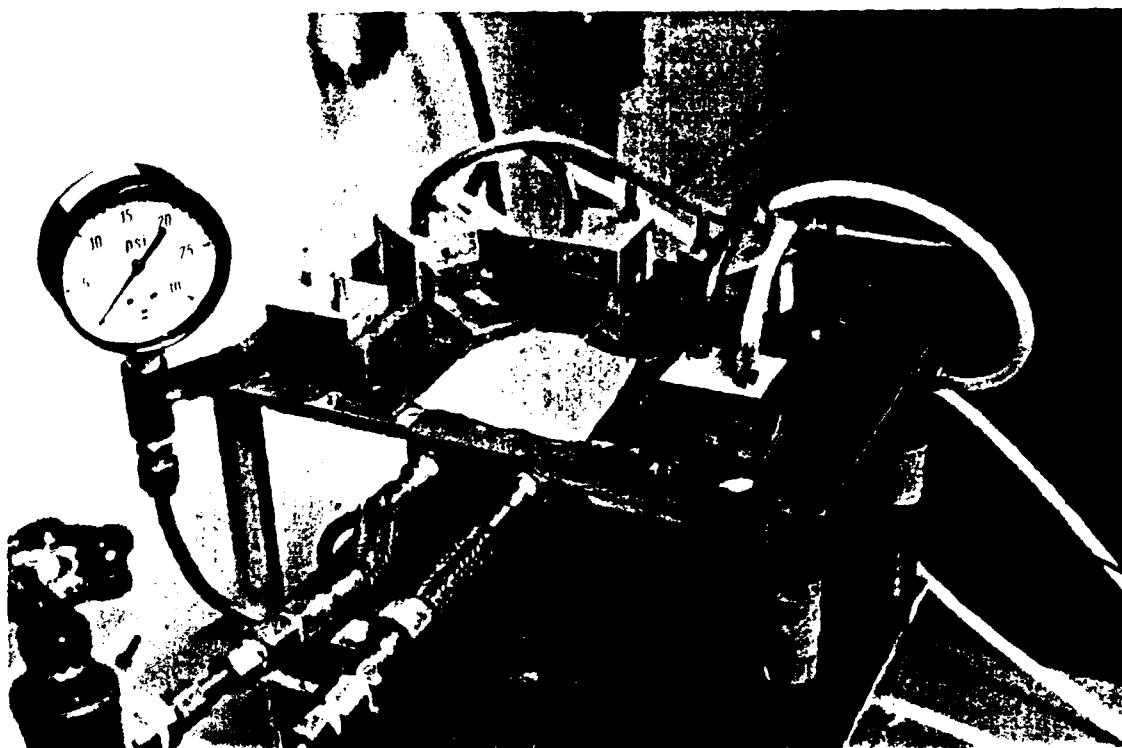


Figure 7. Clemson Folding Unit

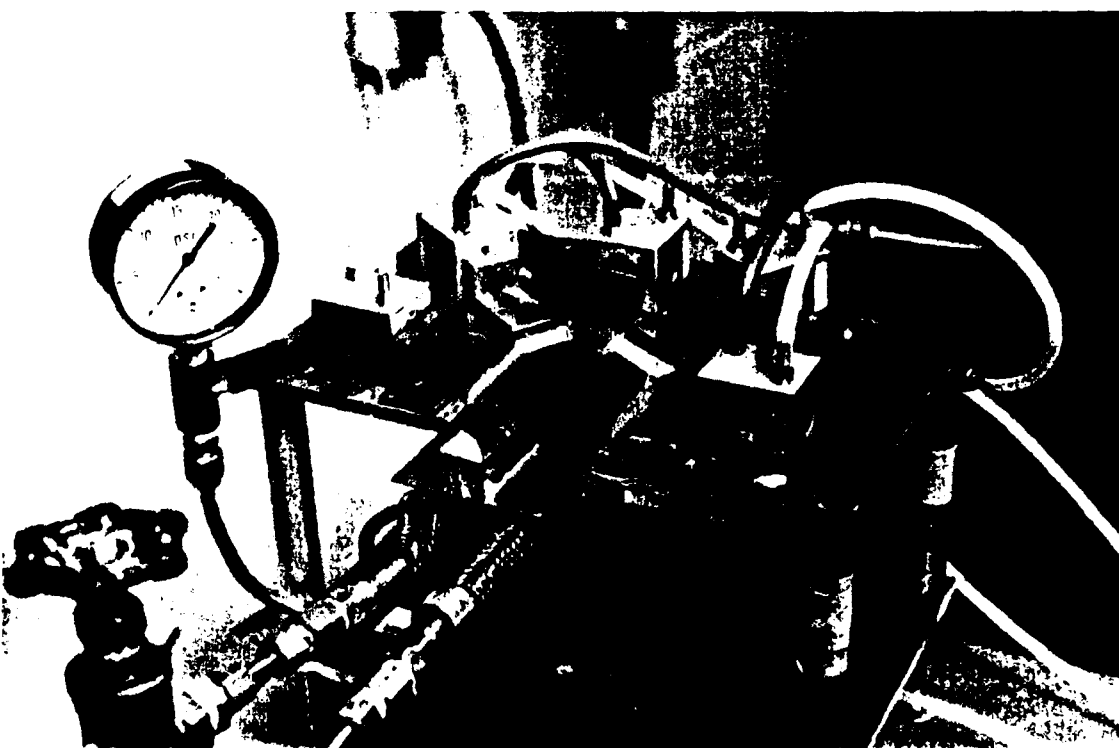


a flow passage which was fed by two steam inlets. The steam flooded the flow passage and was forced through the sintered bronze pressing plate into the cloth.

The selected method of folding consisted of 4 steps which are shown in Figure 8. The folding blades were aligned so that, when in the retracted position, the cloth sample would align itself with the pressing bed, (Figure 8A). The folding mandrel was placed on the sample over the pressing bed, (Figure 8B). The pressing bed assembly was lowered pneumatically to a point about 1/8 inch below the top surface of the stationary top plate. Since the cloth was forced into a smaller cavity, the edges folded upward, also shown in Figure 8b. The blades were extended and the edges of the cloth were folded, (Figure 8C). At this point, the folding mandrel was removed and the pressing bed assembly moved vertically upward to hold the edges of the fabric between the folding blades and the sintered bronze bed. The steam flow was directed into the steam manifold where the steam was forced through the sintered bronze and into the fabric sample. Note that the gauge on the left side of each figure remained unchanged in all photos. This gauge measured the pressure of the steam inside the steam manifold. Since the pressure remained approximately zero, the pressure of the steam inside the manifold was approximately that of the ambient pressure in the laboratory throughout the folding operation.

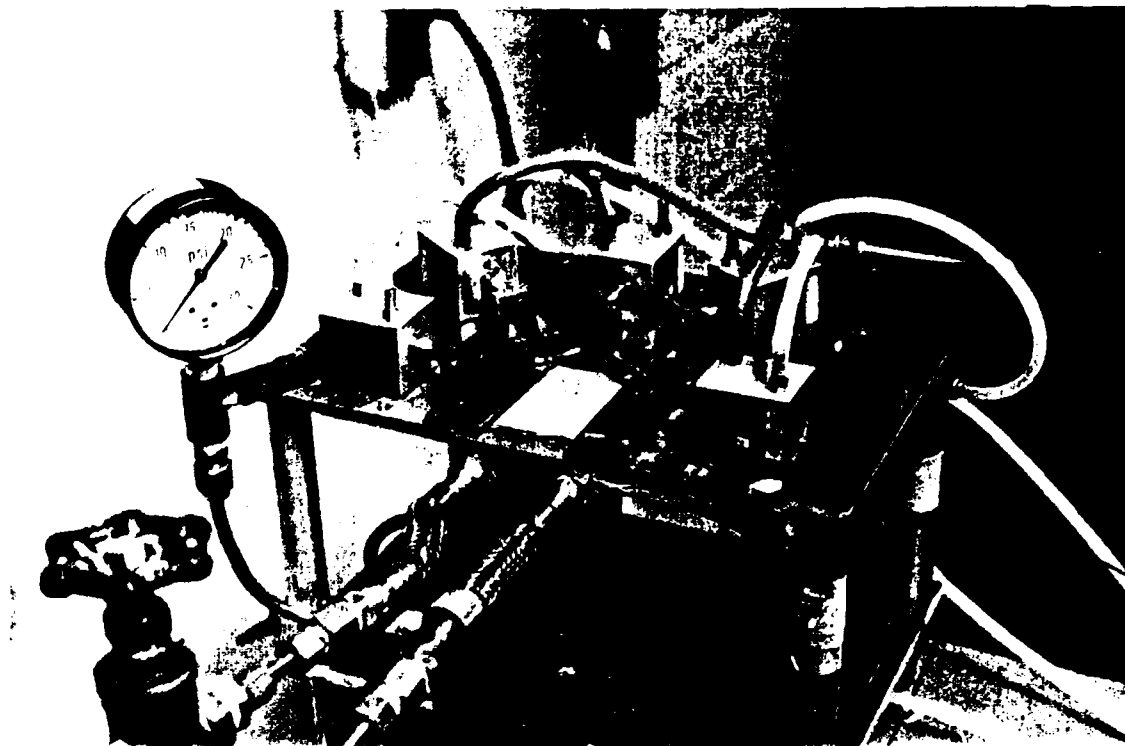


A.

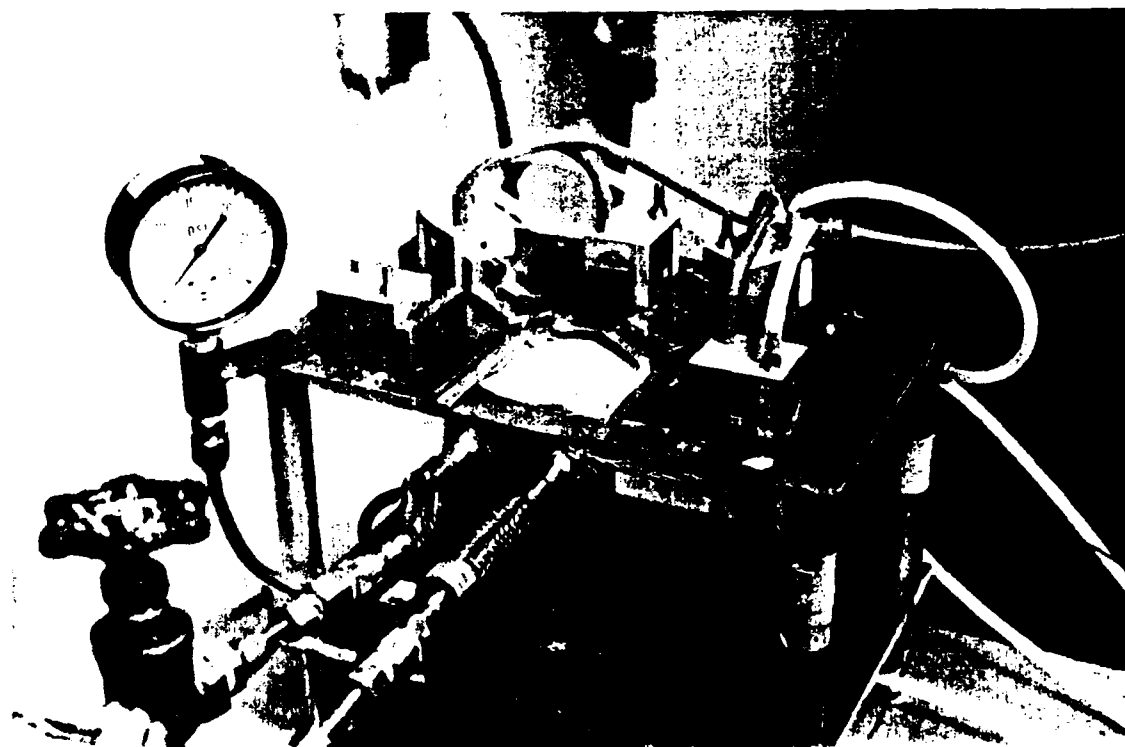


B.

Figure 8. Clemson Folding Operation.



C.



D.

Figure 8. (Continued)

The fabric sample was held in place while being wet, heated, and dried with the superheated steam. The steam flow was then diverted from the manifold, and a vacuum pulled room temperature air through the cloth, sintered bronze, and steam manifold to cool the fabric and the mechanism. The folded fabric sample was removed from the folding unit (Figure 8D).

#### Heat Transfer Analysis of the Folding Unit

In order to assist with the design of the aforementioned proof-of-concept apparatus, an implicit finite-difference computer program was written and used to estimate heat transfer in the fabric and the mechanism. The program was written so that system parameters could be varied, and corresponding heat transfer rates evaluated. The result was a design tool which was used to help determine material types and dimensions in the machine design.

As seen in Appendix C, the finite-difference program modeled the steam flow as one-dimensional. The bed and the cloth were discretized through the thickness, and heat transfer was estimated at each boundary as well as within each material. The temperature as a function of time in each material was obtained by solving a recursive set of partial differential equations using the Thomas Algorithm[2]. The output was an estimate which was used to size system components such as sintered bronze thickness, folding blade dimensions, and steam generator specifications. Appendix C.

shows the program derivation in detail with the actual location of each node and the boundary conditions imposed on the system.

Appendix D gives the actual listing for the one-dimensional implicit finite-difference program. Each of the material properties, the steam properties, and steam flow rates are presented. The sample results shown in Appendix E are indicative of the actual results obtained by using the properties of the actual prototype system. The format of the results shows the temperature at each node within the material at discrete points in time.

The finite-difference program was used as a tool during the design of the mechanism to identify trends in mechanism behavior with regard to heat transfer. By varying mechanism dimensions in the program, variations in heat from the steam to the cloth could be investigated. Sintered bronze dimensions and folding blade dimensions required for adequate heat transfer were estimated through iterative use of the program. The use of these dimensions in the fabrication of the folding unit yielded a proof-of-concept folding unit which operated satisfactorily.

#### System Layout and Operation

Figure 9 shows the system layout for incorporating the superheated steam into the design. Measuring the temperature and pressure of the steam downstream of the superheater completely defined the state of the steam at the inlet to the

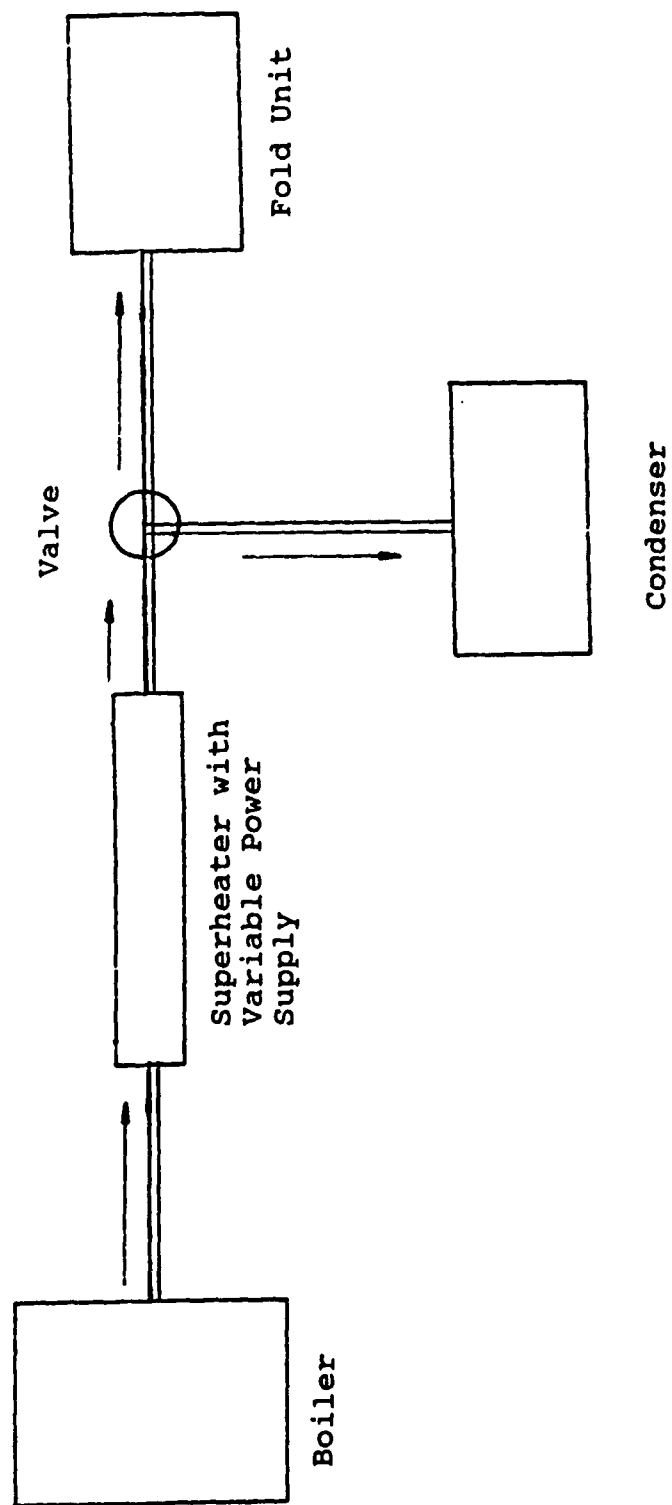


Figure 9. Clemson System Layout

folding machine. This temperature was used to control the output of the superheater and achieve the desired level of superheat in the steam. Increasing or decreasing the power to the superheater changed the state of the steam. Experimental observations were made for varying states of steam over the ranges of folding parameters introduced earlier.

In order for the superheater and boiler to operate at steady state conditions, a valve was placed upstream of the folding unit to divert the flow of steam when the folder was in use (Figure 9). The steam generation and degree of superheat remained constant throughout the folding cycle, even though the steam was not needed for the entire folding cycle. When the steam was in demand, the valve opened to allow steam passage to the folding unit. When the steam was no longer needed, the flow was diverted directly to the condenser.

### Equipment

A Reimers JR Custom steam generator with a 5 lbm/hr capacity and a 1.5 kW heating element was selected for the system. The boiler reservoir held 2.5 gallons of water, thus it would operate for at least four hours producing approximately 20 pounds of steam before refilling was needed.

The steam superheater selected was a Sylvania tube-type fluid heater. The heater was capable of producing superheated steam at temperatures up to 1500°F.

### Jet Sew Design

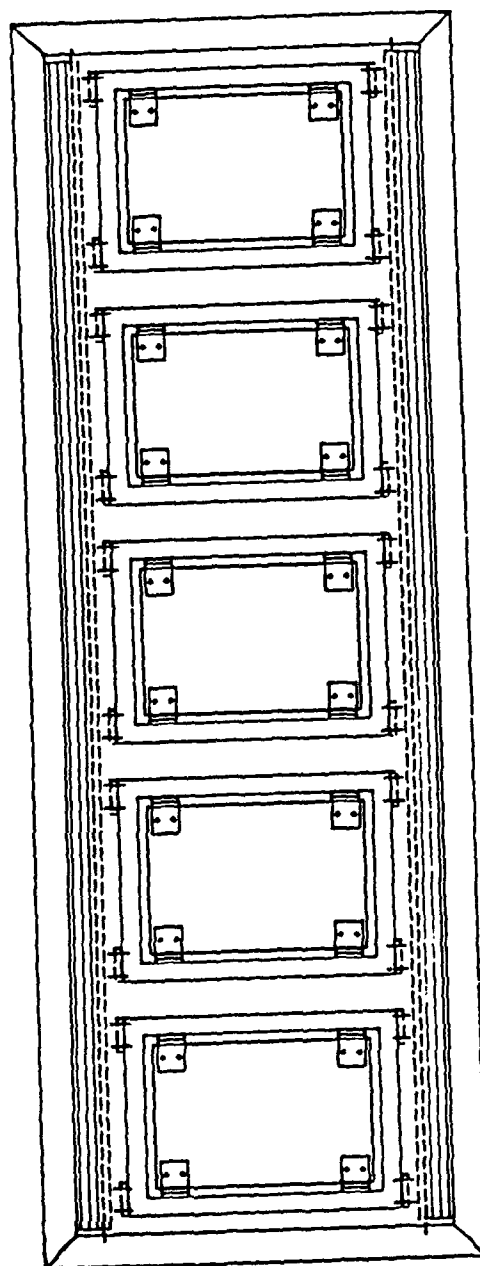
While the Clemson design utilized superheated steam for heating, moisture addition, and moisture retraction, the Jet Sew design utilized conductive heating and cooling with manual moisture addition to fold cloth. This section presents the operating principles and the folding process utilized by the Jet Sew design.

### System Layout and Operation

As seen in Figure 10, the Jet Sew device used five stations to fold cloth. At each station one step in the folding process, i.e., loading, folding, heating, cooling, and unloading, was accomplished. In cases where moisture was required, the moisture was added manually to the fabric prior to loading the fabric at the loading station. The folding unit was mounted to allow it to traverse between stations. A diagram of the folding unit is shown in Figure 11.

The folding process is shown in Figure 12. The cloth was loaded onto the loading station by hand, (Figure 12A). The folding unit traversed to the next station, (Figure 12B) where the mandrel moved vertically downward, forcing the fabric into the folding cavity. The edges of the fabric were held vertically upward by the folding blades. The folding blades were extended, folding the edges of the cloth over the mandrel. The mandrel was removed from the sample, and the bed of the folding cavity moved vertically upward,





Top View

Figure 10. Schematic of Jet Sew System Layout Indicating  
Five Sequential Operating Stations

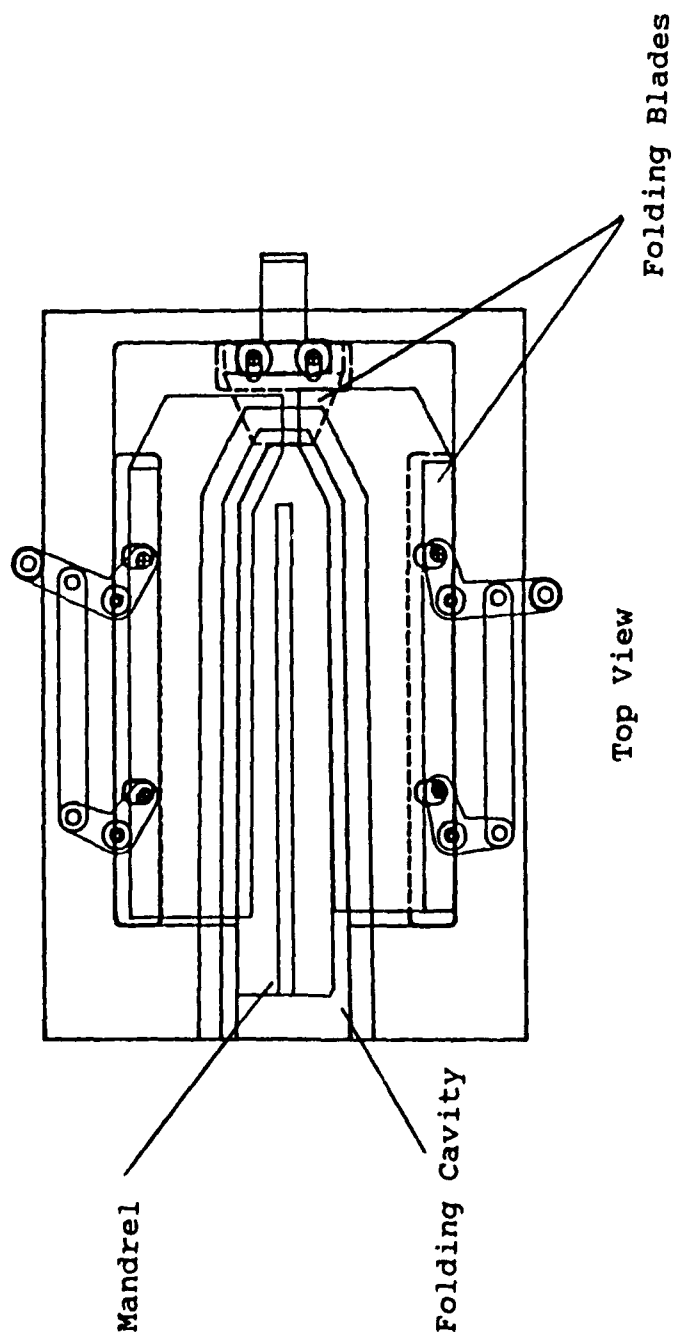
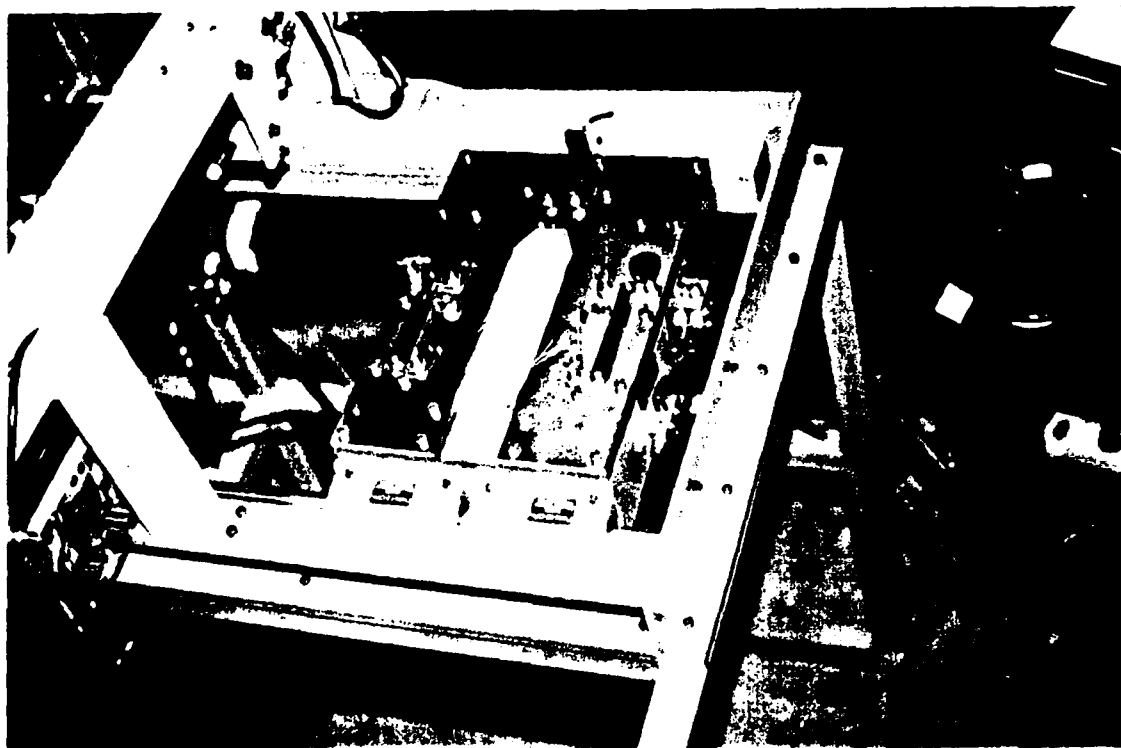
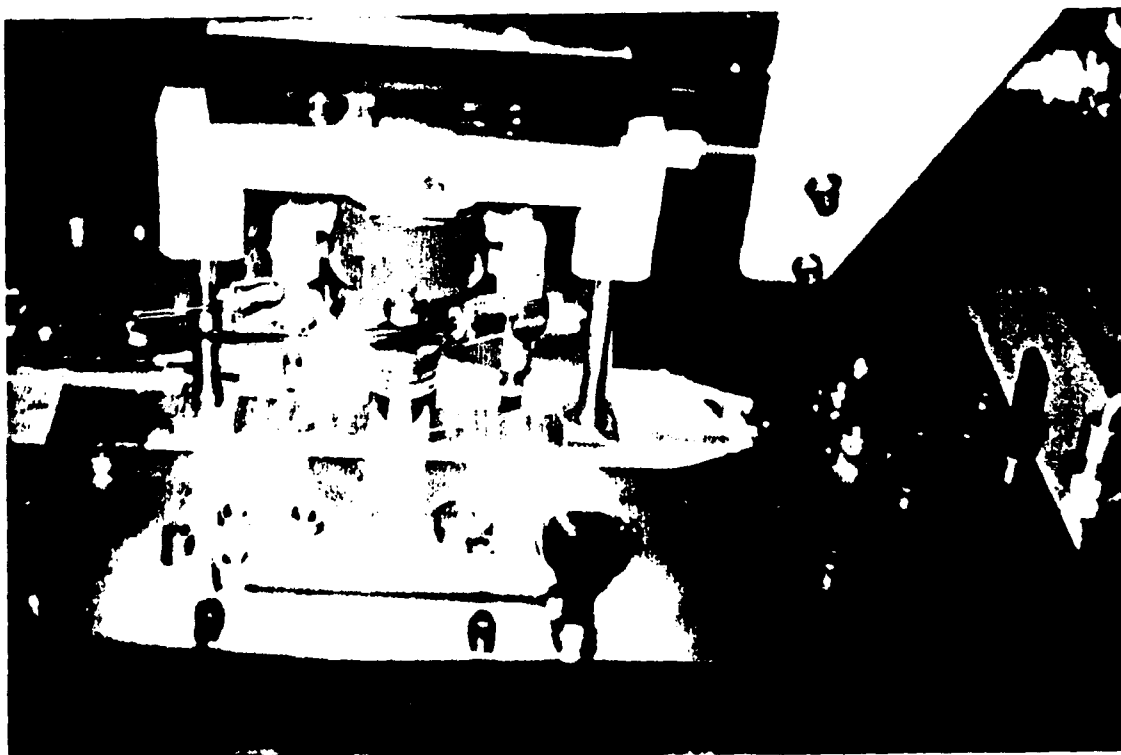


Figure 11. Jet Sew Folding Unit

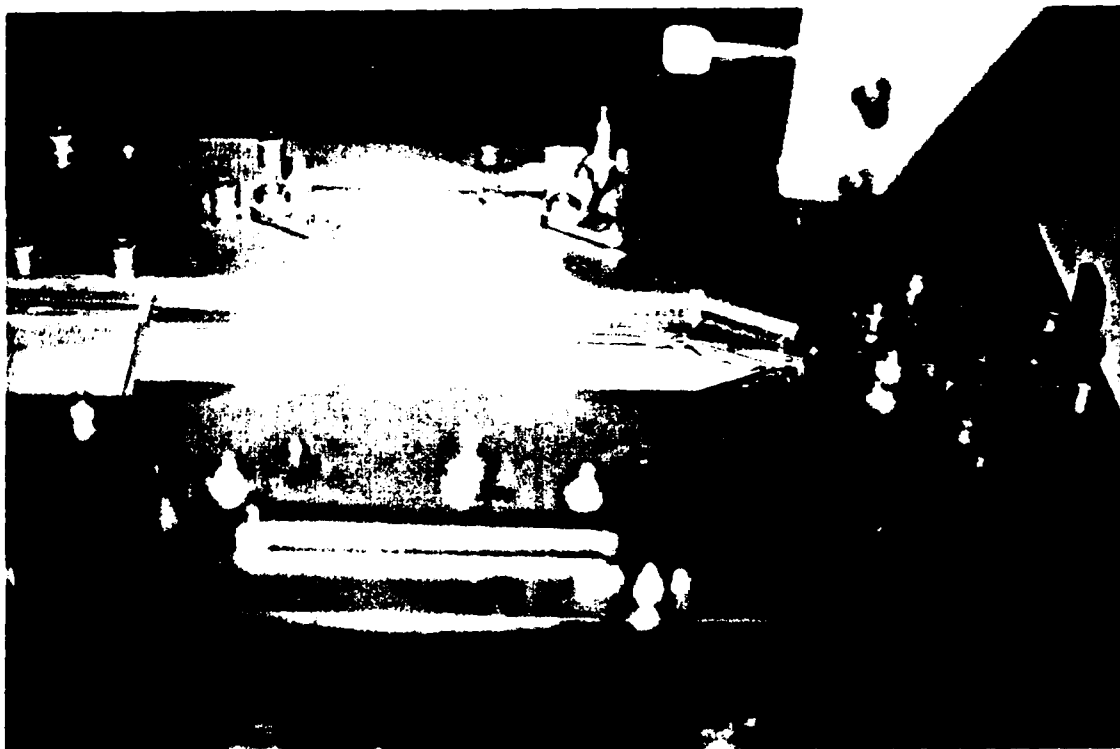


A.

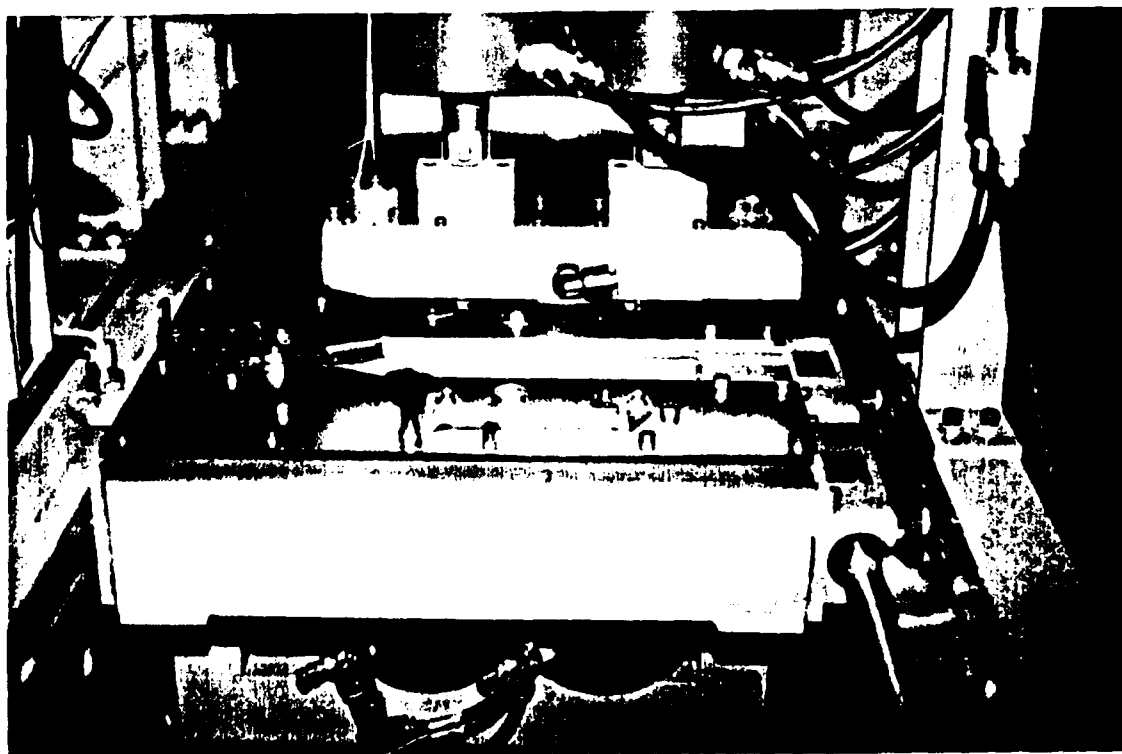


B.

Figure 12. Jet Sew Folding Operation.

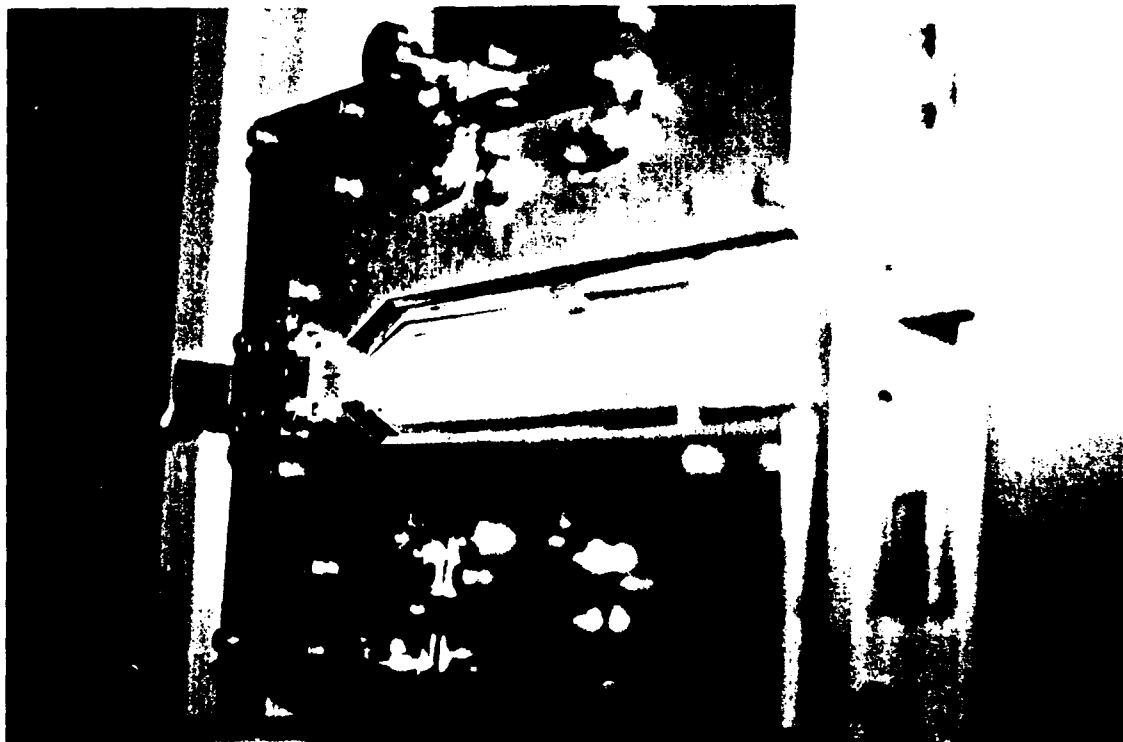


C.



D.

Figure 12. (Continued)



E.

Figure 12. (Continued)

holding the cloth in the folded position between the folding bed and the folding blades (Figure 12C). The folding unit traversed to stations 3 and 4, where the fabric was heated and cooled via hot and cold blocks (Figure 12D). The final step in the folding process was to remove the folded sample from the folding unit at the unloading station (Figure 12E).

### Summary

Chapter III presented each of the two proof-of-concept prototypes which were developed for folding woven fabric samples. The operating principles of each device were explained along with the system layout of each device. Chapter IV will describe the means which were devised to evaluate folded samples. In addition, the experimental methods employed with both mechanisms will be discussed, and the results obtained from each mechanism will be presented.

## CHAPTER IV

### EXPERIMENTAL SETUP AND METHODOLOGY

#### Introduction

The hardware and measuring techniques employed were the same for both mechanisms. J-type thermocouples with an Omni digital multi-readout type 405A were used for measuring temperature in both the Clemson device and the Jet Sew device. Temperature was measured and recorded at several strategic locations in each device to further quantify folding parameters needed for folding cloth. The folding air pressure was also measured to further quantify folding parameters. Pressure was measured in the steam manifold of the Clemson device to provide information regarding steam state incident to the sintered bronze. Each of the two pressure measurements were measured with a Bourdon tube pressure gauge.

Moisture content of each fabric sample containing cotton was measured in both mechanisms with a factory calibrated textometer type DMB from Mahlo America. The moisture meter used several electrodes to assess cloth resistivity to electrical current as the moisture content in the fabric varied.

Folds made by both the Clemson and the Jet Sew device were evaluated using an overhead projection to measure fold characteristics. Criteria for successful folds, measurement techniques used in measuring fold characteristics, as well as experimental methods for each design are discussed in detail

in this chapter. Results obtained for each design are discussed.

### Fold Evaluation

#### Fold Characteristics

The projection of a folded sample placed flat on an overhead projector clearly showed the warp and fill in a single ply of material. Also, the edges of the folded material were easily distinguishable. The resulting projection looks similar to that shown in Figure 13. Since there was such a large contrast between areas of one ply and areas of two plies, and since the projected image was at least 10 times the material size, hand calipers or a scale was used to measure the fold dimensions directly from the overhead screen.

Figure 13 also depicts the dimensions which were measured from a fabric sample. The lengths denoted 'h' and 'dm' were the height of each fold and the length of the projection of each fold to the horizontal, respectively. The actual length of the fold, D, was related to the projection length, dm, by the cosine of the included angle,  $\theta$ . The projection length, dm, was measured directly from the enhanced image of an overhead projector.

Consider the case where a piece of clear plexiglass is placed directly over the top of a folded fabric sample while on the overhead projector. The edge folds would then be pressed to the horizontal, and the actual length of the fold,



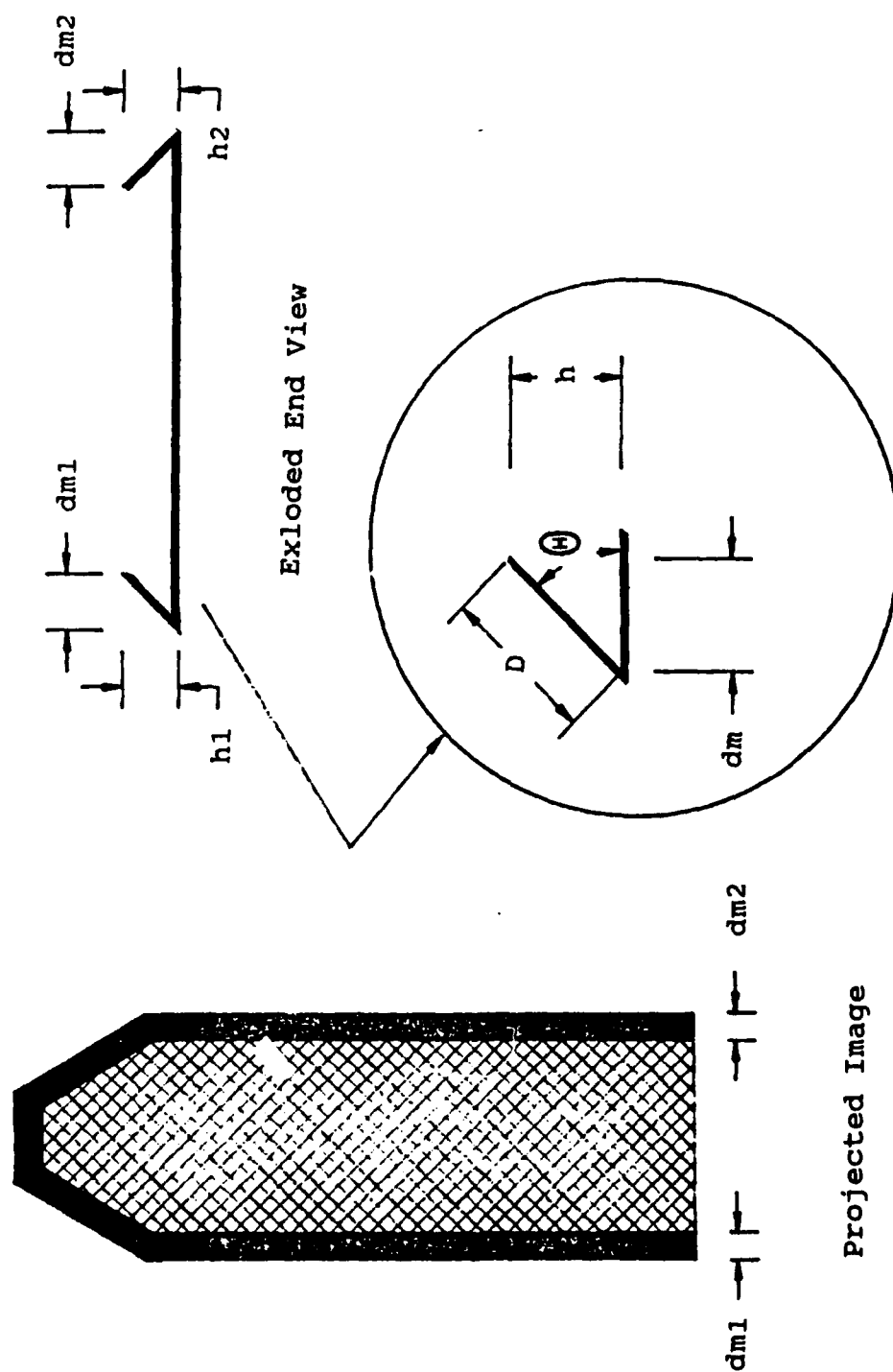


Figure 13. Fold Characteristics

D, could be measured directly from the projector screen. Therefore, the springback angle,  $\theta$ , was calculable from direct measurements of D and dm:

$$\theta = \text{ARCCos} (dm/D).$$

### Springback Ratio

Referring again to Figure 13, note that  $(d_1^2 + h_1^2)^{1/2} + (d_2^2 + h_2^2)^{1/2}$  is equal to the initial width of an unfolded sample minus the width of the folded sample. Hence, denoting the initial width of an unfolded sample as L, and the width of the folded sample as W, we can define a springback ratio such that:

$$[(D_1^2 + h_1^2)^{1/2} + (D_2^2 + h_2^2)^{1/2}] / (L - W) = 1.$$

Typically, an ideal fold would have zero height ( $h_1 = h_2 = 0$ ). Then, the optimum case occurs as  $(h_1 + h_2)/(L-W)$  approaches zero, or  $D_1 + D_2 = L - W$ . By normalizing the springback ratio in this way, it is clear that variations in  $\theta$  and any wrinkles in the edge fold will cause variations in the values of  $dm_1$  and  $dm_2$ , causing the value of the springback to be less than 1.

Using the first two terms of the Taylor's Series Expansion as an approximation for the cosine function, consider:

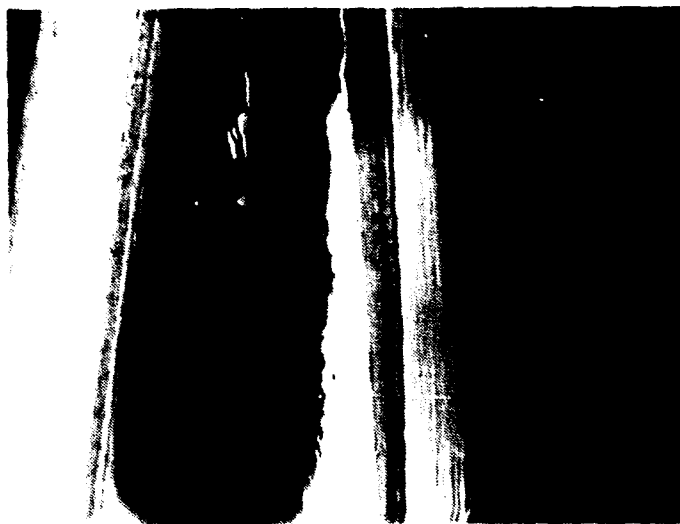
$$\cos\theta = 1 - \theta^2/2!.$$

It is obvious that the springback ratio approaches 1 very quickly at small angles of  $\theta$ , since  $dm/D = \cos(\theta)$ .  $dm/D = 0.9962$  for  $\theta = 5^\circ$ , and  $dm/D = 0.9848$  for  $\theta = 10^\circ$ . The

difference in  $\cos 5^\circ$  and  $\cos 10^\circ$  is only 0.0114. Therefore, resolution becomes an important source of error in the measurements. Consider  $D=0.250\text{in}$  and  $\theta = 5^\circ$ , then  $dm$  would have to be measured at  $0.249\text{in}$ . Hence, resolution of  $\theta$  in  $5^\circ$  increments requires a resolution of  $dm$  of  $0.001\text{ in}$ .

Comparing known dimensions on the folded sample with dimensions taken from the screen, a projection factor can be obtained. A projection factor can be defined as the amount which an image is magnified by the overhead projector. In these measurements, a projection factor of 10 was used. Therefore, every inch of fabric sample appeared as 10 inches on the overhead screen. As a result, a resolution in  $dm$  of  $0.001\text{in}$  translates to a  $0.010\text{in}$  resolution on the screen. A resolution of  $0.010\text{in}$  can be obtained easily with hand calipers or a scale graduated at  $1/100$  of an inch.

In this research, a successful fold was defined as a fold with: (1) a single, definite crease line (V-shaped vs. U-shaped fold), and (2) an angle between the edge fold and the sample body of less than  $10^\circ$ . Figure 14 shows a cross-section of several folds as seen using a Zeiss EL Microscope with a magnification factor of 4. Figure 14A shows the cross-section of a successful fold, i.e., a fold with a springback angle of  $10^\circ$  or less. Note the definite V shape of the fold, indicating a definite crease at the origin of the angle. In contrast, Figure 14B shows an unsuccessful fold. Not only was the springback angle greater than  $10^\circ$ , but the fold has a U shape, indicating no definite creases



A.



B.

Figure 14. Cross-sections of Actual Folds as Seen Under Microscope (4X). A. Good Fold B. U-shaped Fold C. Edge Fold Wrinkle



C.

Figure 14. (Continued)

in the fabric. Figure 14C shows a fold with a wrinkle on the edge fold itself. The vertical line superimposed on the picture provides a straight reference for contrast. A fold with a wrinkle was considered unacceptable, and was readily noted from visual observation and the projection techniques described above.

### Experimental Methods

The objectives of experimentation with both devices, i.e., the Clemson device and the Jet Sew device, was to illustrate the folding process for woven fabrics, to establish temperature, moisture, pressure, and time relationships required in folding woven fabrics, and to provide a basis for comparison between two possible mechanisms designed and fabricated for folding woven fabrics. In order to meet these objectives, both mechanisms were tested using the same fabrics and the same measurement systems. Both mechanisms were evaluated using the criteria for successful folds as defined earlier. The purpose of this section is to provide a detailed presentation of the methods employed in experimentation for both the Clemson device and the Jet Sew device.

#### Clemson Device

As can be seen from the data presented in Appendix I, the following data was documented for each type of fabric tested:

- (1) steam temperature - the temperature of the steam measured in the manifold flow path during folding;

(2) manifold wall temperatures - temperatures taken at two locations within the manifold to monitor heat transfer to and from the manifold;

(3) bronze temperature - the temperature of the bronze bed taken during folding;

(4) drying time - the amount of time required during the influx of superheated steam for 100% cotton or cotton/polyester blends to dry to the moisture content of room conditions after being wet by the superheated steam;

(5) heat time/cool time - amount of time that was required to heat or cool 100% polyester or cotton/polyester blends to the desired temperature level, respectively;

(6) cycle time - the calculation of the cycle time varied depending on the type of material, but normally the cycle time was the summation of the heating and cooling times;

(7) folding pressure - the pressure of the compressed air supplied to the pneumatic cylinder actuating the pressing bed in the vertical direction, measured by Bourdon tube;

(8) cooling temperature - the temperature in polyester or cotton/polyester blends to which the fabric was cooled after folding; and

(9) moisture content - mass of water contained in the cloth expressed as a percentage of the mass of the dry cloth, calculated as:

$$\text{moisture content} = [(\text{mass wet}) - (\text{mass dry})] / (\text{mass dry}).$$

The moisture content was measured directly with a factory calibrated textometer, type DMB, from Mahlo America.

The operator individually varied the steam temperature, cooling temperature, and hence, moisture content for each fabric in the proof-of-concept apparatus until a marginally acceptable fold was produced. The production of a marginally acceptable fold was determined subjectively by the

operator. At the production of a marginally acceptable fold, the operator began varying only the cooling temperature (for the case of 100% polyester or cotton/polyester blends). The cooling temperature was varied until a threshold was reached where the best possible fold was produced for a given steam temperature and folding pressure. The steam temperature was increased or decreased and then held constant while the cooling temperature was varied again. As a result of this process, a given cooling temperature was found as an optimum for a given type of cloth. Then, the steam temperature was varied while holding this cooling temperature constant.

The folding pressure was held relatively constant at 25 psi for each fold so that the effects of heating, cooling, and moisture content could be noted readily. Data was recorded while holding the cooling temperature and folding pressure constant and varying the steam temperature. Each test was repeated for varying steam temperatures, and hence varying manifold and bronze temperatures, heating, cooling, and drying times. The cooling temperature was held relatively constant for each run with the same type fabric, providing direct results regarding heating temperatures, heating times, cooling times, and fold characteristics.

Appendix I also lists the fold dimensions which were measured in accordance with the procedures discussed earlier in the section entitled "Fold Evaluation". To reiterate the conclusions of that section, a successful fold was determined as a fold having a springback angle,  $\theta$ , less than or equal



to 10°, no wrinkles in the edge fold itself, and a definite crease line (V-shaped vs. U-shaped fold).

#### Jet Sew Device

The Jet Sew device was operated and evaluated using the same criteria for successful folds as the Clemson device. The same fabric types were used with both mechanisms. Data was measured and recorded for the Jet Sew device in the same manner as was the Clemson device.

Heating and cooling temperatures, folding pressure, cavity temperatures upon heating and cooling, and cycle times were documented for each type of fabric tested and are presented in Appendix J. The heating temperature and cooling temperature were the temperatures of the heating and cooling blocks at the start of each cycle, respectively. Operating temperatures of the heating and cooling blocks nominally fluctuated 2°, but no more than 10°F, during the cycle.

The fold tests were conducted for constant temperatures of hot and cold blocks and a constant folding pressure. Cavity heating temperature, cavity cooling temperature, and moisture content (in some cases) were varied. The cavity heating temperature, CHT, and the cavity cooling temperature, CCT, were the temperatures of the folding cavity measured at the press bed/fabric sample interface during heating and cooling, respectively. These temperatures varied with the length of time that the fabric sample remained in contact with the

heating or cooling block. The folding pressure was maintained at the maximum pressure obtainable from the compressed air source. The effects of heating, cooling, and moisture were readily noted by holding the folding pressure constant. Holding the hot block temperature constant allowed direct comparison of cycle times for each type of fabric tested.

The heating and cooling times were recorded as the time required to bring the cavity temperature to the desired level during the folding process. The cycle time was taken as the summation of the heating and cooling times. The time to load or unload the fabric sample and the time between stations in the folding process were purposely neglected in calculating cycle time since these times were directly related to the actions of the operator. However, every effort was made to achieve consistency on the part of the operator.

The fold dimensions of each fabric sample were measured as explained earlier. Data was recorded at two different times. First, the data was taken as the fabric sample was removed from the machine and was recorded in the upper left corner of each of the boxes in each data set in Appendix J. Then, after a period of approximately 24 hours, the data was recorded again, as seen in the lower right corner of each box for each data set in Appendix J.

## Discussion of Results

### Clemson Device

All of the raw data sets which are discussed in this section are located in Appendix I. Data set 1 for 100% polyester shows acceptable folds can be created at steam temperatures as low as 305°F, with a minimum cycle time of 25 seconds. Folds made at higher temperatures required essentially the same cycle times. However, steam temperatures above 315° caused some of the fabrics to shine in the area of the fold. The cloth was cooled to a temperature of approximately 290° in each case.

Data set 2 is for 70% polyester and 30% cotton. The 70/30 blend was tested over a steam temperature range of 325-360°F. The optimum fold (zero springback angle) was produced at a steam temperature of 350°F with a maximum moisture content of 13% measured 2 seconds after the steam was directed into the fabric sample. Acceptable folds were made at steam temperatures as low as 345°, and at temperatures as high as 360°F. Each fold was cooled to approximately 290°F. Cycle times noted for acceptable folds were longer than 55 seconds.

Data from the tests conducted on 55% polyester and 45% cotton was assembled in data set 3. Acceptable folds were produced for steam temperatures as low as 350°F, with cooling temperatures of about 295°. The minimum cycle time for creating successful folds was approximately 40 seconds. The moisture content was measured over time and graphed for the

optimum case. The optimum fold was produced at a steam temperature of 355°, with a maximum moisture content of 12.8%, with a cycle time of 41 seconds.

Data set 4 presents the data obtained for fabric blends of 65% cotton and 35% polyester. The cooling temperature was approximately 300°F. Acceptable folds were produced at steam temperatures of 350-355°, while optimum folds were produced at temperatures of about 360°. Maximum moisture content for optimum folds occurred at approximately 2 seconds and were measured near 14.5%. Optimum cycle times ranged from 42 to 49 seconds.

The final data was obtained for 100% cotton fabric. Flat folds occurred at steam temperatures as low as 320°F, with a maximum moisture content of approximately 17%. Drying time, however, decreases with increasing steam temperature, as expected. Therefore, cycle times were reduced for successful folds from near 60 seconds to 28 seconds at increased steam temperatures. Moisture content remained within 1.0 of 17%. Steam temperatures up to 340° were used in folding the 100% cotton fabric.

The effect of decreasing cycle time with increasing steam temperature is not seen as readily in blends containing both cotton and polyester, since additional heating is needed to relax polyester fibers for folding. Thus, the time required for the additional heating caused overall increased cycle times at increased steam temperatures in some cases for blended fabrics.

### Jet Sew Device

All raw data referenced in this section is contained in Appendix J. It is evident from data set 1 for 100% polyester that this material was easily folded. The CHT was varied over a range of 200 to 250°F. The CCT was held constant at approximately 160°F. Each fold produced zero springback angle. The cloth did have a tendency to become shiny around the fold at temperatures above 230°F. However, temperatures as low as 200°F were used to create excellent folds with no shining. Successful folds were created with only a 40° temperature difference in heating and cooling, resulting in a total cycle time of only 15 seconds.

Data set 2 is for folding fabric samples of 70% polyester and 30% cotton. The 70/30 blend was tested over a CHT range of 200-220°F. The CCT range was from 130 to 160°. Raising the CCT to 160°, caused the resulting fold to be unsuccessful. Successful folds were also obtained at CHT values lower than 220°, indicating that the 70/30 blend could be folded over a wide range of heating temperatures, namely 200-220°F. However, it appeared from the data that cooling temperatures of less than or equal to 150° were necessary, since cooling to any temperature higher than 150°F created an unsuccessful fold. Therefore, optimum operating conditions occur for a CHT range of 200-220°F with a CCT of about 150°F. Total cycle times for successful folds range from 20-60 seconds.

Blends containing 55% polyester and 45% cotton were tested and the data was compiled in data set 3. CHT ranged from 210 to 240°F, and CCT values ranged from 150-160°F. All of the runs reported in this data set created successful folds. The shortest total cycle time of 32 seconds occurred with a CHT of 210°F and a CCT of 150°F, thus producing a temperature difference of only 50°.

Data set 4 presents the data obtained for folding blends of 65% cotton and 35% polyester. The presence of more cotton in the blend translates to higher cycle times for folding, indicating higher resistance to heat penetration and higher resistance to creasing on the part of the cotton. Adding moisture to the fabric prior to creasing was necessary to relax the cotton fibers. Adding moisture was found to increase the cycle times because additional time was needed in the heating cycle to evaporate the moisture. The 65/35 cotton polyester blend was folded successfully with a cycle time of 68 seconds, using a CHT of 230°, a CCT of 160°, and a moisture contents of 21%.

The final type of fabric tested was 100% cotton. As seen in data set 5, the addition of moisture was again necessary to relax the cotton fibers. Slightly higher moisture contents were found to be necessary for 100% cotton than were previously reported for the 65/35 blend. The 100% cotton fabric was successfully folded with a moisture content of 24%, a CHT of 230°, a CCT of 150°, at a cycle time of 80 seconds. To reiterate a point made earlier, the use of

progressively higher moisture contents increases the time needed in the heat cycle due to the evaporation of the moisture. Therefore, with higher percentages of cotton and higher moisture contents, higher cycle times were encountered.

### Comparison of Results

The limiting values of the folding parameters are summarized for comparison in Tables II and III. The Jet Sew device operated at cycle times as low as 15 seconds in the case of 100% polyester, while the Clemson device operated at cycle times on the order of 20 seconds. The data showed that the 100% polyester was relatively easy to fold, and comparable cycle times were recorded for each machine. In contrast, the 70/30 polyester/cotton blend showed a difference of cycle times by a factor of two. The Clemson device reported cycle times in excess of 60 seconds while the Jet Sew device produced comparable folds on the order of 30 seconds. The 55/45 polyester/cotton blend was folded with cycle times of 40-45 seconds using both the Jet Sew and the Clemson devices.

The case of the 65/35 cotton/polyester blend indicated that increasing amounts of cotton forced drastic increases in cycle times in using the Jet Sew device. The Jet Sew device recorded cycle times near 70 seconds while the Clemson device produced comparable folds with cycle times as low as 42 seconds. For the case of 100% cotton fabric, cycle times for the Jet Sew device ranged from 80-111 seconds in producing

marginally acceptable folds, while the Clemson device produced optimum folds in as little as 28 seconds. Hence, it appears that the Jet Sew device was more suited to folding fabrics containing higher polyester content, while the Clemson device was more suited to folding fabrics of high cotton content.

Table II. Limiting Values of Folding Parameters for Clemson Device

Material	Moisture Addition	Heating Temp (F)	Cooling Temp (F)	Pressure (psi)
100% Cotton	17%	338		25
65/35 Cotton/ Polyester	14%	360	305	26
55/45 Poly./ Cotton	13%	348	298	25
70/30 Poly./ Cotton	13%	344	290	26
100% Polyester	0%	310	292	25
Uncertainty	+/- 0.22%	+/- 2.75°F	+/- 2.75°F	+/- 2.1psi



Table III. Limiting Values of Folding Parameters for Jet Sew Device

Material	Moisture Addition	Heating Temp (F)	Cooling Temp (F)	Pressure (psi)
100% Cotton	24%	230	150	20
65/35 Cotton/ Polyester	21%	230	160	20
55/45 Poly./ Cotton	--	220	170	20
70/30 Poly./ Cotton	--	200	150	20
100% Polyester	--	200	160	20
Uncertainty	+/- 0.22%	+/- 2.75°F	+/- 2.75°F	+/- 2.1psi

Note from Tables II and III that folding temperatures reported for the Clemson device were markedly different than those reported for the Jet Sew device. The Jet Sew device employed the more conventional means of pressing, i.e. conduction, and the folding temperatures were comparable to those reported for conventional safe ironing temperatures. In using superheated steam, however, reported folding temperatures were nominally lower than those reported for conventional ironing.

The folding parameter set, which included temperature, pressure, and moisture content was defined for each mechanism, though there was some discrepancy in reported quantities between the two mechanisms. Hence, the chosen method of heating, cooling, and moisture addition and retraction provided a variety of data by which each type of fabric sample could be folded.

CHAPTER V  
CONCLUSIONS AND RECOMMENDATIONS

Introduction

Both the Clemson device and the Jet Sew device used similar techniques for mechanically folding the fabric samples. The Jet Sew device did not make provisions for moisture addition, thus making the device inadequate for fabric samples containing high cotton content. Manually adding moisture allowed the Jet Sew device to successfully fold the fabric samples fabric samples containing a high cotton content. Hence, successful folds were produced by both mechanisms for each type of fabric tested.

The cost of operation of each unit was comparable. The major operating cost was due to the power consumption for heating the hot blocks in the Jet Sew device, and for producing and superheating the steam in the Clemson device. The estimated steady-state power consumption of the Jet Sew device was 1.5 kW, based on the cartridge heaters that were chosen for use in heating the hot block. The estimated steady-state power consumption for the Clemson device was 1.75 kW, though this figure varies directly with the degree of superheat supplied to the steam by the superheater.

Since neither mechanism was a production unit, comparing the units on the basis of cost of fabrication would be purely conjectural, and in the opinion of the author, would not .

contribute a fair evaluation of either mechanism.

Therefore, the only logical means of comparing the two mechanisms objectively with the existing information was on the basis of cycle time.

### Conclusions

Both the Clemson device and the Jet Sew device produced successful folds in each type of fabric tested, even though moisture had to be manually added in the use of the Jet Sew device to fold fabrics containing high cotton content. In comparing the results obtained for each mechanism, it was obvious that relatively high cotton content in the fabric samples caused drastic increases in cycle times for the Jet Sew device due to the additional time needed to evaporate the moisture from the fabric. Contrarily, fabric samples containing higher polyester content were more easily folded using the Jet Sew device. Hence, it appeared that the entire range of cotton/polyester blend fabrics could be folded optimally using some combination of the methods employed by each mechanism.

With the addition of moisture, it would be possible for the Jet Sew device to fold the entire range of cotton/polyester blend fabrics. However, as previously mentioned, the trade-off is increased cycle times over the superheated steam method. It may also be possible, upon further investigation, to modify the Clemson design to better accommodate those fabric blends with high polyester content. Since the

Clemson device successfully folded 100% polyester, it appears that only a slight modification of the existing machine would yield satisfactory results using the Clemson device.

The next step in the design of a marketable folding mechanism would be to use the results obtained here to iterate the process, that is, to modify the original design of each mechanism to optimize folding for the entire range of cotton/polyester blend fabrics used in shirt manufacture today.

#### Recommendations

In retrospect, it seems that the discrepancy in the results between the Clemson device and the Jet Sew device may have occurred due to the measurement techniques employed in each device. A more accurate approach to obtaining the temperature of the cloth sample would have been to measure the temperature of the cloth between the edge folds.

One obvious means of improving the Clemson device would be to devise a means of exhausting the superheated steam after it flows through the cloth. This would make the mechanism more safe and would help limit condensation to areas of the cloth, the folding bed, and the folding blades. In deriving a production unit from the Clemson device, the folding mandrel and blades would need to be redesigned to accommodate a full-size collar band as opposed to the fabric samples used in testing. A mandrel is currently used in collar band folding and fixing which collapses to retract

from the folding cavity without disturbing the edge folds or the folding blades.

Similar adjustments could be made to the Jet Sew device in deriving a production unit. The folding mandrel and blades would have to be redesigned in the same way that the Clemson design would. The Jet Sew device must also be made to accommodate moisture addition in order to successfully fold fabrics containing a high cotton content.

Both the Jet Sew and the Clemson device were designed to be manually operated for test purposes, however, one notable improvement could come through automatic controls. Each machine has been designed so that controls could be added in future models.

It is the opinion of the author that a production folding unit should make use of the superheated steam technique described in this thesis. The superheated steam lowered the cycle times involved with high cotton content materials considerably over the use of purely conductive heating. Also, the use of a more efficient cooling technique should improve the mechanism's performance in those materials containing high polyester content. For this reason, the initial phase of continued research should include the investigation of further improvements to the cooling system employed with the Clemson device to determine whether or not the use of superheated steam may be further refined to be more efficient in folding high polyester content materials.

## APPENDICES

Appendix ATabulated Safe Ironing Temperatures

<u>Fiber</u> <u>Class</u>	<u>Type</u>	<u>Moisture</u> <u>Regain</u>	<u>Claimed Safe</u> <u>Ironing Temp.</u>	<u>Recommended</u> <u>Ironing Temp.</u>
cotton	regular	7.0 %	360°F	425°F
	mercerized	8.5	360	425
polyester	Dacron 54	0.4	356	325
	Dacron 64	0.8	325	325
	Fortrel	0.4	356	325
	Kodel 200	0.2	425	350
	Kodel 400	0.4	356	325
	Mylar Film	0.0	300	325
	Vycron 2	0.6	350	300
	Vycron 5	0.4	350	325

Moisture regain is expressed as a percentage of the moisture free weight at 70°F and 65% humidity.



Appendix B  
Generation of Alternatives

Alternative 1

The first configuration, depicted in Figure B-1, utilizes a collapsible device, called a mandrel, for holding the fabric in place during folding. Also, alternative 1 utilizes conductive heating and cooling blocks for the addition and extraction of heat. The cavity is constructed of phenolic composite to insulate the cavity from extensive heat transfer.

Figure B-2 indicates the eight steps of operation. First, the pressing block recedes to form a cavity with the phenolic walls. Then, the mandrel pushes the cloth into the cavity forcing the edges of the cloth to fold upward. The blades then extend, folding the cloth edges down into the cavity. The mandrel collapses in step 4, and then retracts in step 5. Step 6 shows the placement of a heating block, applying pressure simultaneously with the pressing block. Finally, in step 8, the cooling block is placed atop the folding blades, and once again pressure is applied simultaneously with the pressing block.

Several disadvantages should be noted with the use of this configuration. First, since the folding blades must remain intact during the entire operation to hold the cloth, provision must be made for the heating and cooling of the blades. This creates several problems, two of which are .

1	Phenolic Cavity Wall
2	Pressing Block
3	Collapsible Mandrel
4	Folding Blades

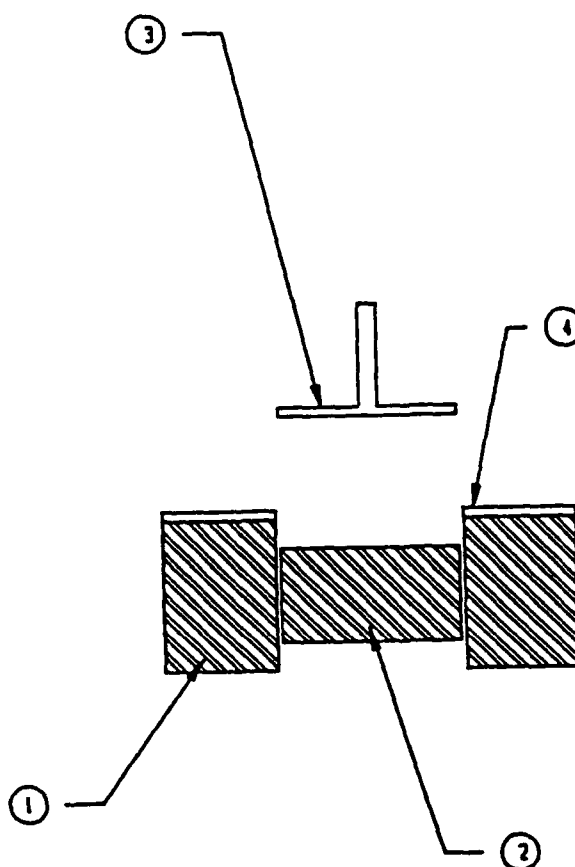


Figure B-1. Alternative 1. Cross-section of Folding Cavity

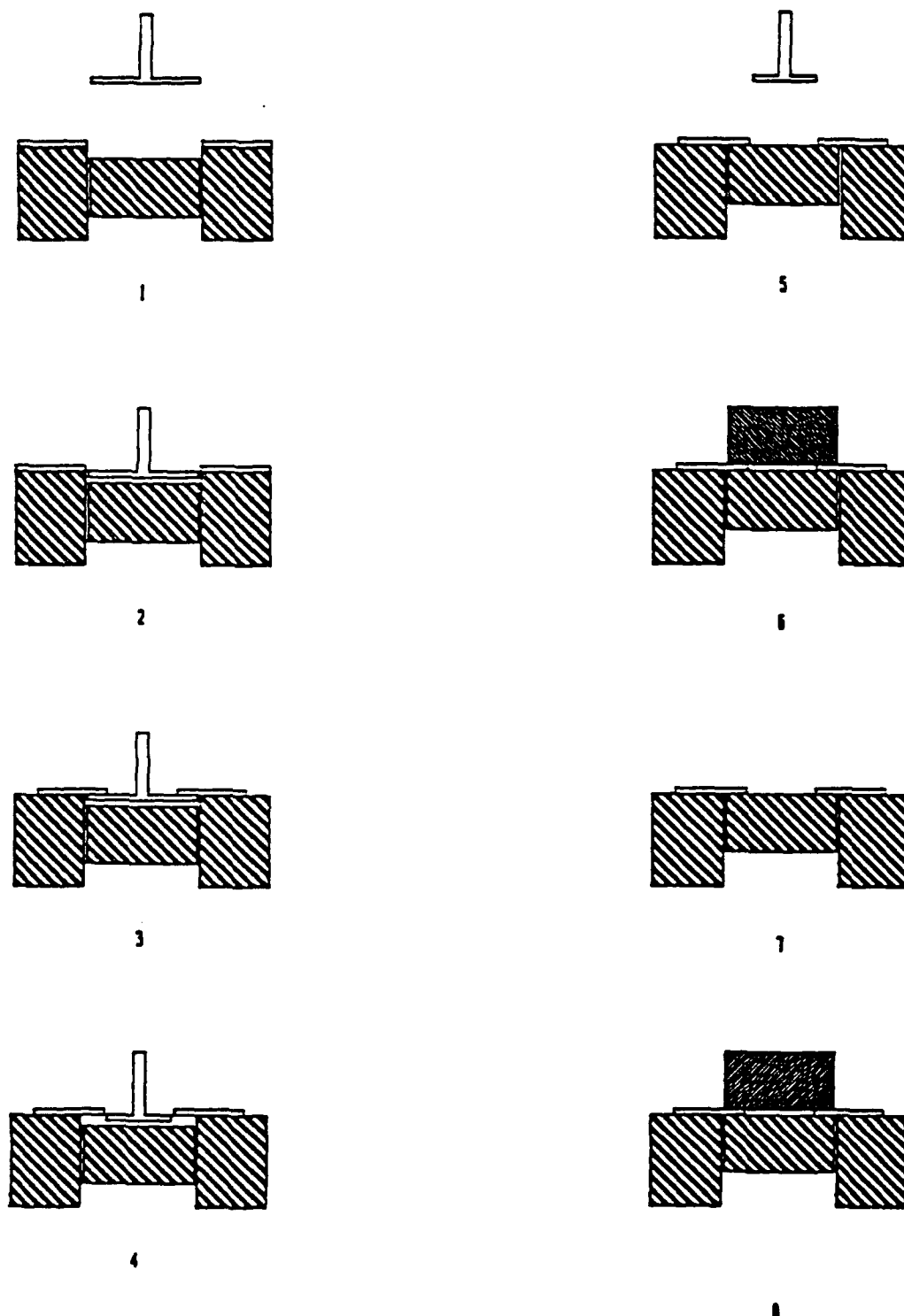


Figure B-2. Alternative 1. 8 Steps of Operation with Heating and Cooling through Blades

immediately apparent: (1) there will be loss of heat due to the contact resistances between the block and the blades, and (2) repeated thermal cycling of the blades could lead to thermal fatigue. To avoid excessive heat losses and thermal gradients, the blades should then be made as thin as possible. This might effectively eliminate the problems at hand, however, in pressing the material, the heating or cooling block must then be applied at precisely the same time and at precisely the same pressure as the pressing block, since reducing the cross-section of the blade has also eliminated any structural capabilities.

#### Alternative 2

In an attempt to alleviate the potential heat losses associated with the blades of alternative 1, a derivative of the first alternative is shown in Figure B-3. This second alternative employs a thin, flexible membrane to form the base of the folding cavity. As seen in Figure B-4, the folding operation is much the same as presented for alternative 1, with a few notable exceptions.

The membrane mandates the application of heating and cooling from the under side of the machine. There is no longer the heat loss associated with heating and cooling the blades, but rather the heat loss of a thin membrane. However, the blades must now have structural capabilities to support pressure from the blocks beneath. Also, the use of

1	Phenolic Cavity Wall
2	Heating / Cooling Block
3	Collapsible Mandrel
4	Folding Blades
5	Thin Membrane

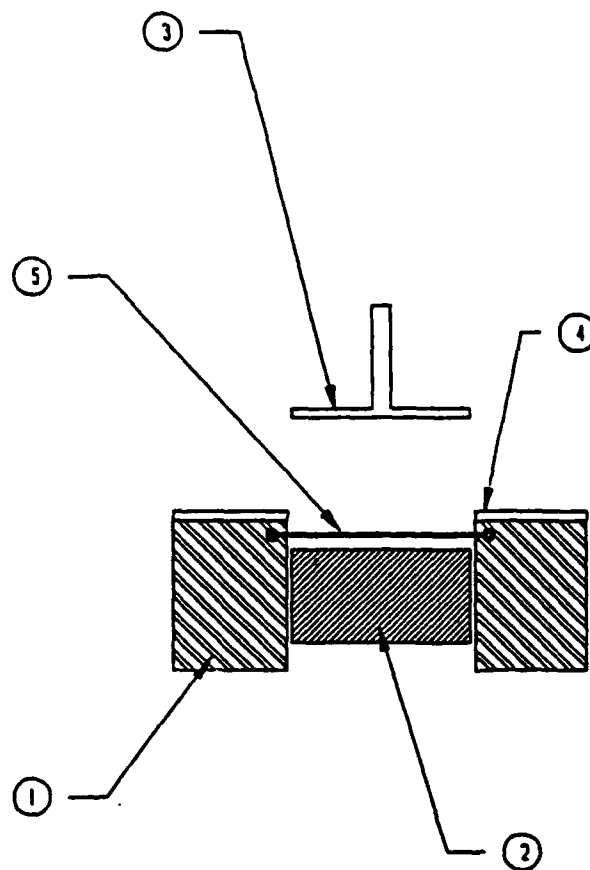


Figure B-3. Alternative 2. Cross-section of Folding Cavity

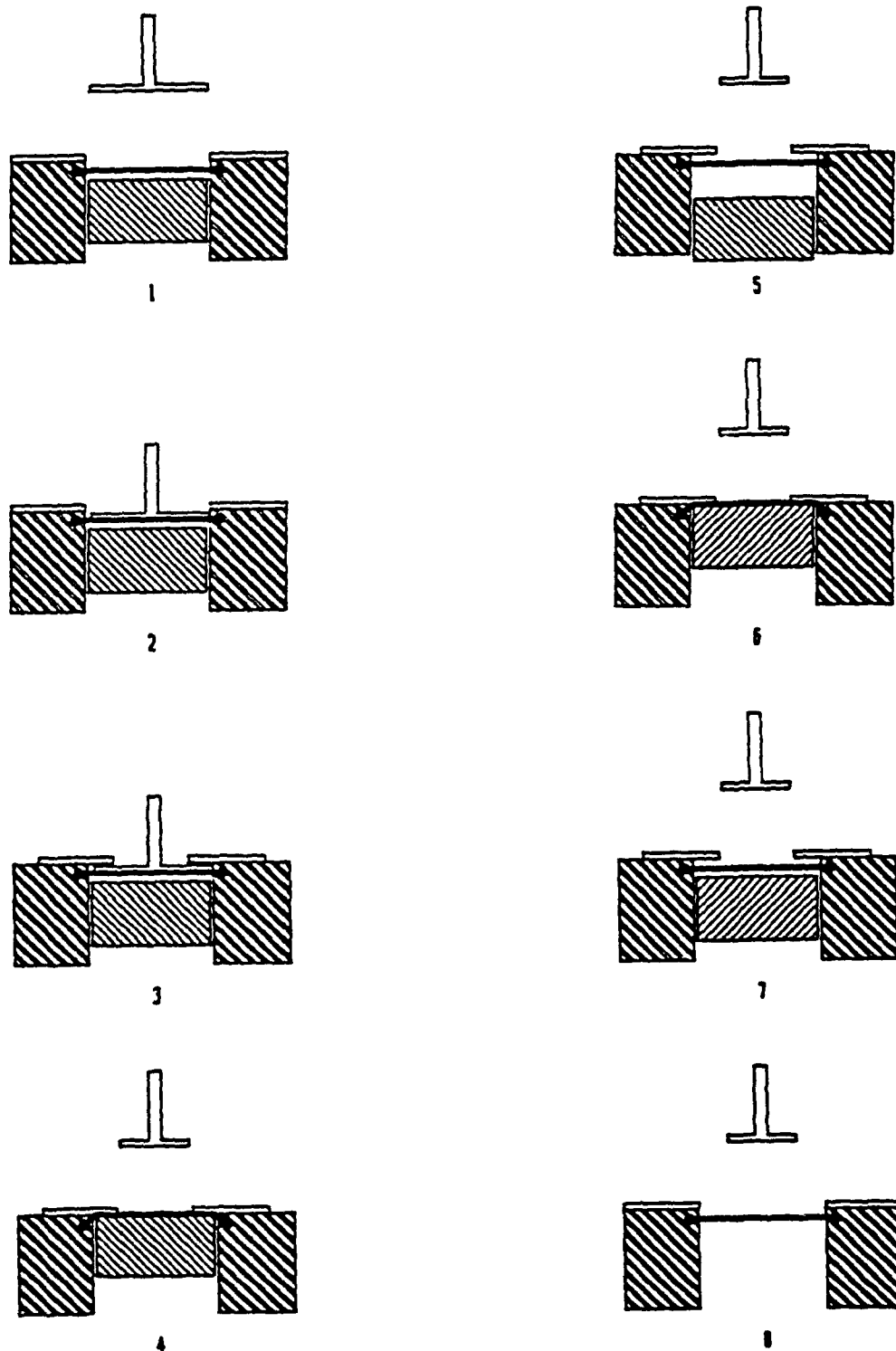


Figure B-4. Alternative 2. 8 Steps of Operation with Heating and Cooling through Thin Membrane

the membrane complicates any adjustment of the cavity depth which must occur for accommodation of varying fabric thicknesses.

### Alternative 3

Figure B-5 shows the configuration and major components of alternative 3. As a means of conserving energy by not heating unnecessary material, this configuration introduces a multi-stage cavity design where heating and cooling occur only along the edges of the material.

Figure B-6 illustrates the stages of operation. The first five steps are similar to those described for the previous two alternatives. The mandrel has a dual purpose as shown in step 6. After the fabric has been heated and pressed (step 5), the expanded mandrel then acts as a punch and replaces the blades by holding the cloth, then it pushes the pressing bed to the second level of the cavity for cooling (step 8).

This alternative has the advantage of alleviating the thermal cycling in the machine. Also, only the edges of the fabric are heated, which indicates a lower power consumption. Nonetheless, the fabric handling problems associated with retracting the blades and replacing them with the mandrel were never overcome. The fabric must be completely supported at all times, and this alternative configuration proved inadequate in this regard.

1	Phenolic Cavity Wall
2	Heat Source
3	Heat Sink
4	Steel Heating Zone
5	Collapsible Mandrel / Press
6	Pressing Bed
7	Folding Blades

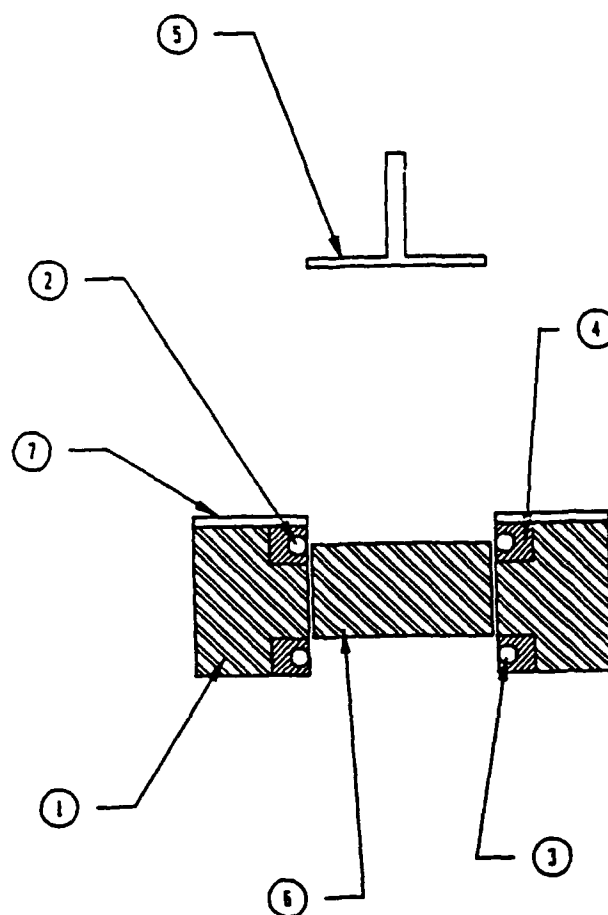


Figure B-5. Alternative 3. Cross-section of Folding Cavity



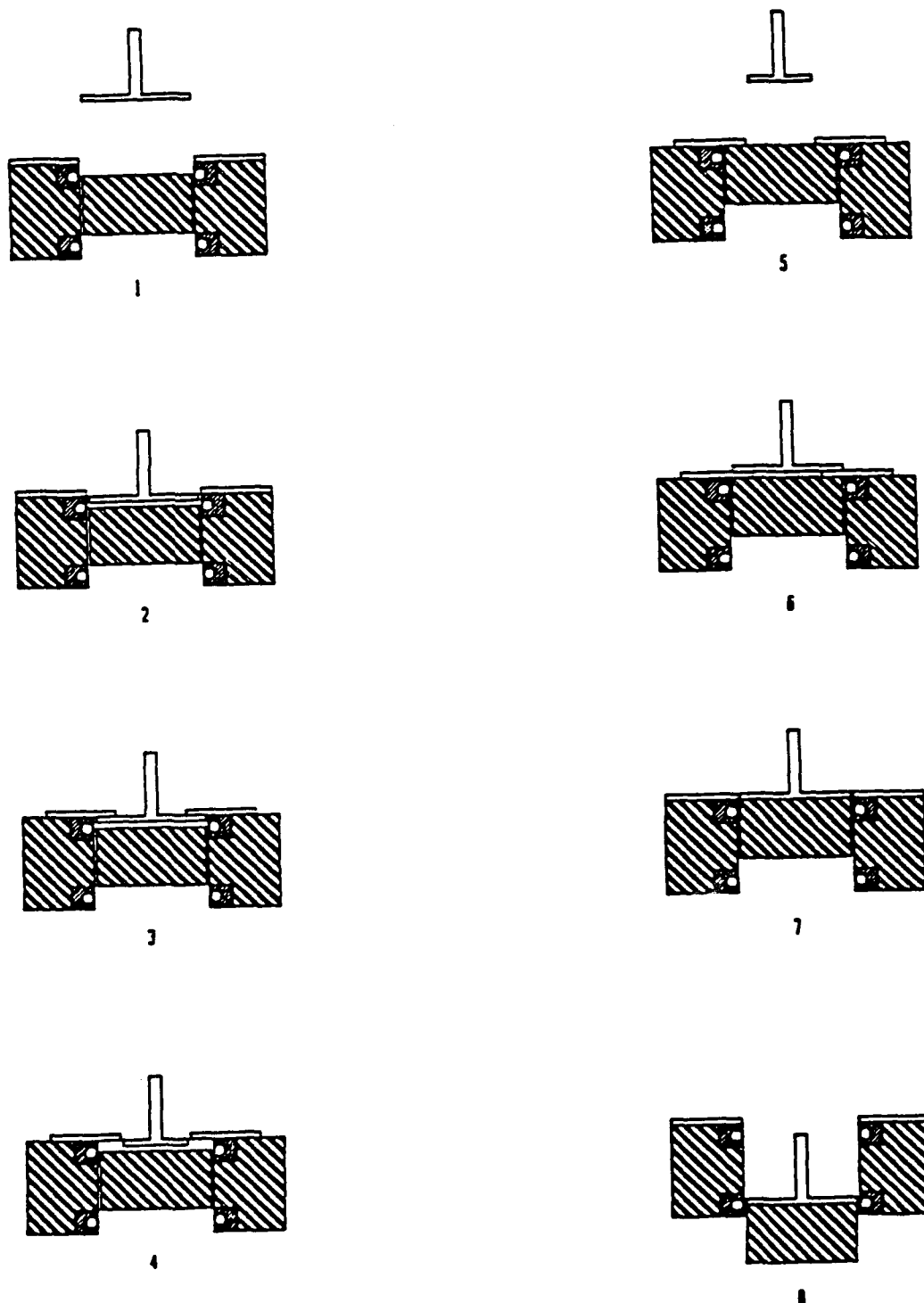


Figure B-6. Alternative 3. 8 Steps of Operation with Multi-stage Folding Cavity Using Heating and Cooling Stations

#### Alternative 4

Figure B-7 illustrates an alternative configuration which was considered in an attempt to solve the fabric handling problems associated with alternative 3. This alternative uses the multi-station cavity as before, but a stationary lip replaces the folding blades. As seen in Figure B-8, the mandrel expands while in the cavity, forcing the cloth under the lip. The fold is completed when the pressing bed pushes upward in step 5. The remainder of the operations are as described earlier.

This alternative, in actuality, does not eliminate the fabric handling problems discussed earlier. In fact, additional handling problems are encountered in steps 2 and 3. First of all, the action of the cloth cannot be predicted as it is forced through the cavity opening of step 2. Second, a problem was encountered in forcing the centerline of the fabric cross-section to coincide with the centerline of the cavity cross-section, i.e., positioning within the cavity is uncertain.

1	Phenolic Cavity Wall
2	Heat Source
3	Heat Sink
4	Steel Heating Zone
5	Collapsible Mandrel / Press
6	Pressing Bed

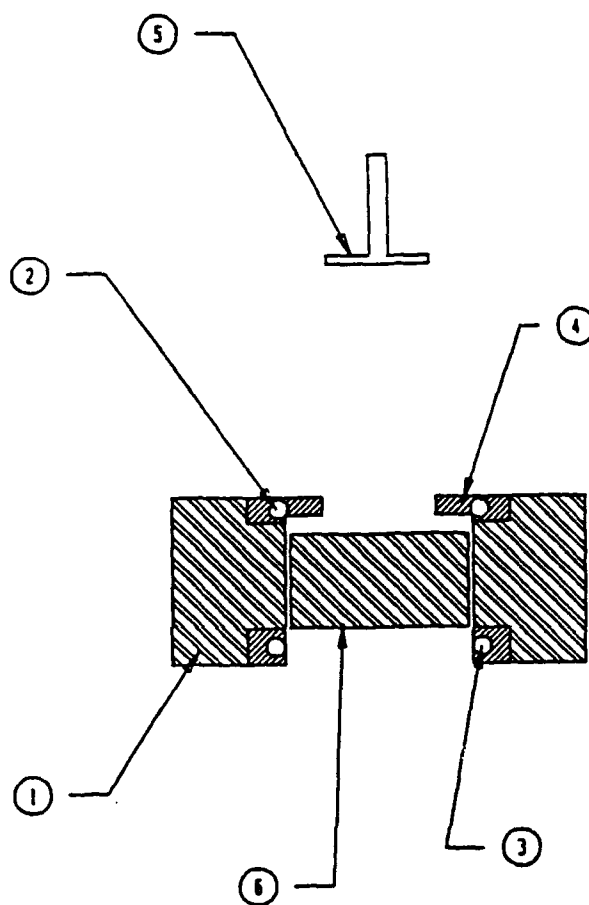


Figure B-7. Alternative 4. Cross-section of Folding Cavity

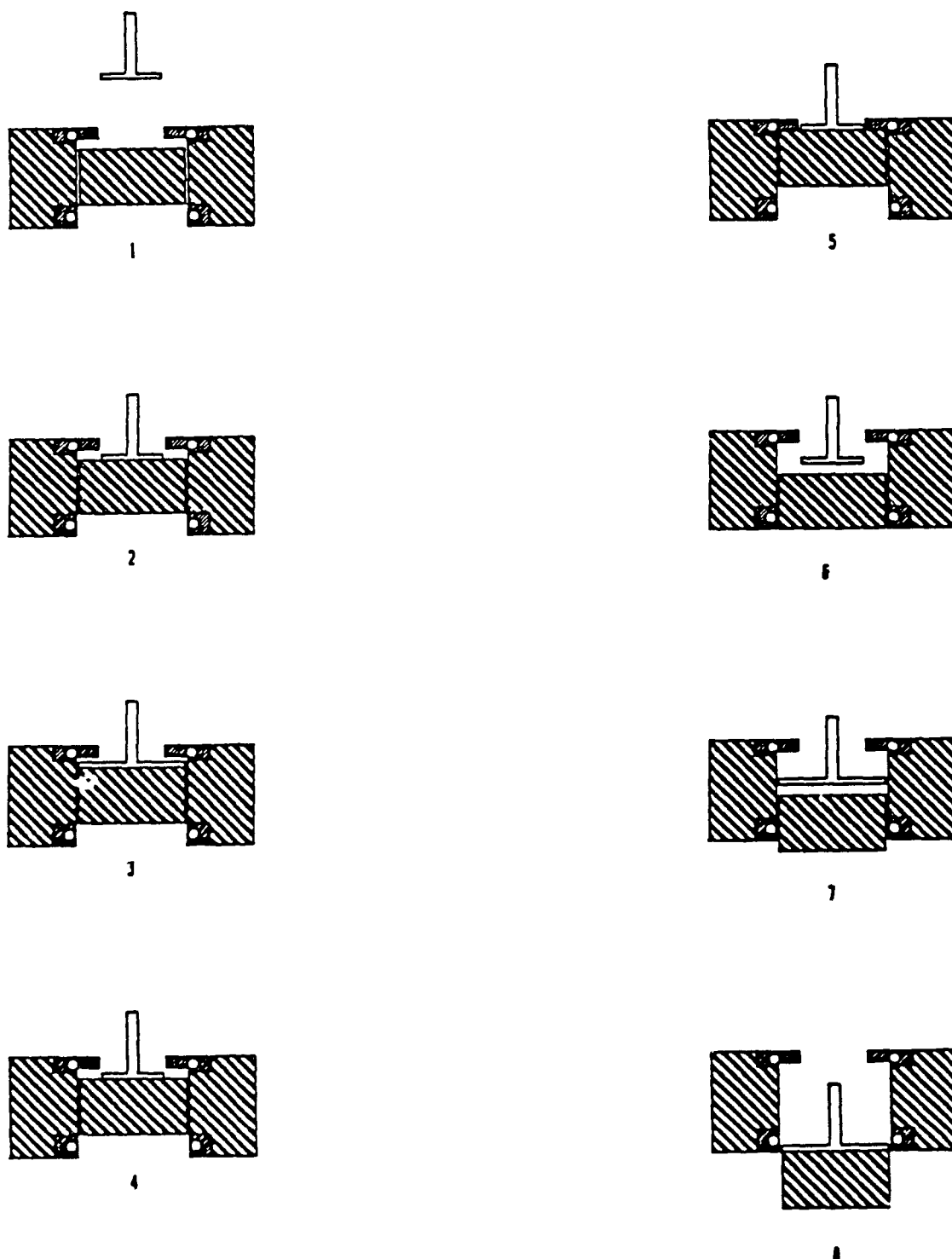


Figure B-8. Alternative 4. 8 Steps of Operation with Modified Mandrel Design

### Appendix C

#### Heat Transfer Analysis - Implicit Finite-Difference Model

The folding bed was modeled using a one-dimensional finite-difference model. The temperature distribution for the sintered bronze and the fabric was modeled using a single-phase equivalent model for heat transfer processes in packed beds[3]. The Conservation of Energy equations for both the solid phase and fluid phase of a packed bed were used in deriving the single-phase equivalence of a two-phase system. By assuming that the second derivative of the temperature of the fluid with respect to position is equal to the second derivative of the temperature of the solid with respect to position, a single-phase equivalent partial differential equation can be derived which is volume-averaged for the porous medium and the superheated steam. The error introduced by assuming the second derivatives to be equal is small in the superheated steam system.

The discretized energy equations were derived in one-dimensional form by performing an energy balance at each spatial location in the system[4]. Figure C-1 shows the grid layout for the finite-difference method and the boundary conditions present in the system.

The application of the equivalent single-phase model to the sintered bronze and the fabric results in the following energy equation:

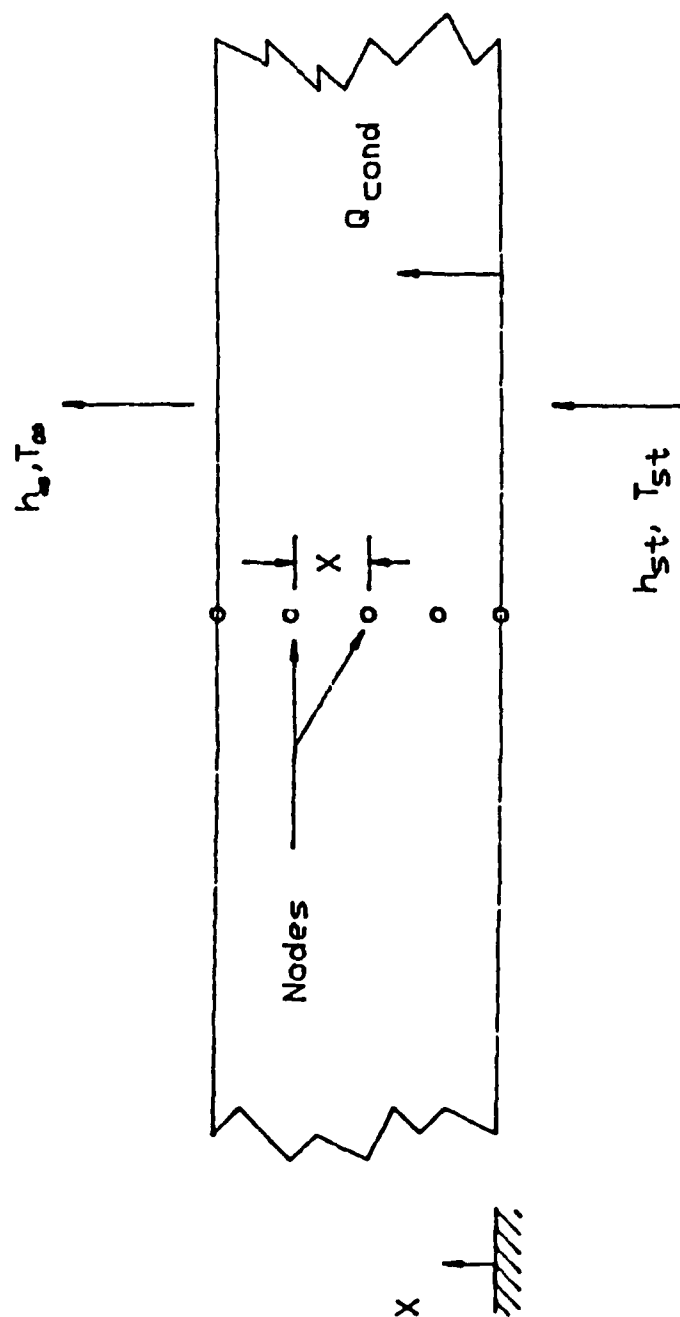


Figure C-1. Cross-section of Porous Material Indicating Elemental Discretization and Boundary Conditions

$$(1-\epsilon)\rho_s C_s \frac{\partial \theta}{\partial t} = \lambda_{ax} \frac{\partial^2 \theta}{\partial x^2} - m_f C_f \frac{\partial \theta}{\partial x}$$

$\lambda_{ax} = \lambda_o + m_f^2 C_f^2 / ha =$  axial effective thermal conductivity (kcal/m sec °K)

$\epsilon$  = void fraction

$C_s$  = solid heat capacity (kcal/kg °K)

$\rho_s$  = solid density (kg/m<sup>3</sup>)

$C_f$  = fluid heat capacity (kcal/kg °K)

$\theta$  = solid temperature (K)

$T$  = steam temperature (K)

$h$  = convection coefficient related to average particle temperature (kcal/m<sup>2</sup> sec °K)

$a$  = sintered bronze particle unit surface area per unit volume estimated as  $6(1-\epsilon)/d$  for spheres

$d$  = diameter of the beads which make up the sintered bronze (m)

$m_f$  = mass flow rate of steam (kg/sec).

The transient energy equation was then discretized and solved using the one-dimensional finite-difference method[4]:

$$(1-\epsilon)\rho_s C_s (T_i^{n+1} - T_i^n) / \delta t =$$

$$\lambda_{ax} [(T_{i+1}^{n+1} - 2T_i^{n+1} + T_{i-1}^{n+1}) / \delta x^2]$$

$$- (M_f C_f) [(T_i^{n+1} - T_{i-1}^{n+1}) / \delta x]$$

$i$  = node specification

$n$  = time specification

$\delta t$  = time step

$\delta x$  = change in position.

Heat transfer from the steam to the blades can be estimated in a similar fashion by utilizing the one-dimensional finite-difference technique. By performing a heat balance on a single blade, and assuming negligible conductive losses, the

energy equation can be written in discretized form as follows:

$$T_i^n =$$

$$T_i^{n+1} [1 + 2\alpha/\delta_x^2] - \alpha/\delta_x^2 [T_{i+1}^{n+1}] - \alpha/\delta_x^2 [T_{i-1}^{n+1}]$$

where  $\alpha$  is  $[S/(k C_S)]$

$k$  is the thermal conductivity of the solid

$C_S$  is the solid specific heat.



Appendix DProgram Listings for Implicit Finite-Difference Model  
of Porous Materials and Steel Folding Blades

C THIS PROGRAM USES THE IMPLICIT FINITE DIFFERENCE METHOD  
 C OUTLINED IN INCROPERA & DEWITT, FUNDAMENTALS OF HEAT AND  
 C MASS TRANSFER, SECOND EDITION, TO DETERMINE THE TEMPERATURE  
 C DISTRIBUTION WITHIN CLEMSON UNIVERSITY'S DESIGN OF A COLLAR  
 C BAND FOLDING DEVICE. 1-D EXPRESSIONS ARE USED, AND HEAT  
 C TRANSFER RELATIONS ARE USED FOR SOLID POROUS MEDIA ACCORDING  
 C TO D. VORTMEYER AND R. J. SCHAEFER, EQUIVALENCE OF ONE- AND  
 C TWO-PHASE MODELS FOR HEAT TRANSFER PROCESSES IN PACKED BEDS:  
 C ONE DIMENSIONAL THEORY, CHEMICAL ENGINEERING SCIENCE, 1974,  
 C VOL. 29, PP. 485-491.

```

      *  DIMENSION A(50),B(50),C(50),T(50),VEC(50),A1(50),B1(50)
        ,C1(50),T1(50),VEC1(50)
      REAL KSTEAM,MF,KC,KS
      INTEGER P
      OPEN (unit = 5, file = 'lpt1')
      DELT=0.1
      TSTEAM = 415.0
      KSTEAM=4.8E-6
      KS=0.013
      KC=9.57E-6
      NNOD=5
      NNODC=5
      DP=0.0005
      DPC=0.0077
      VF=.3
      VFC=.5
      ROS= 539.
      ROC=4.9
      CS=0.1
      CC=0.311
      MF=0.001389
      CF=0.47
      ABRONZE=6*(1-VF)/DP
      ACLOTH=6*(1-VFC)/DPC
      HFC=0.00087
      HC=0.00087
      H=0.013
      AX=KS+MF**2.*CF**2./(H*ABRONZE)
      AXC=KC+MF**2.*CF**2./(HC*ACLOTH)
      XLEN=.125/12.
      XLENC=.05/12.
      DELX=XLEN/(NNOD-1)
      DELXC=XLENC/(NNODC-1)
      CONST=(1.-VF)*ROS*CS
      CONSTC=(1.-VFC)*ROC*CC
      TAIR=70.

```

C  
 C  
 C

INITIALIZE MATRICES

```

      DO 1 I=1,NNOD
        A(I)=0.0
        B(I)=0.0
        C(I)=0.0
        VEC(I)=70.0
1      CONTINUE

```

```

      DO 2 I=1,NNODC
        A1(I)=0.0
        B1(I)=0.0
        C1(I)=0.0
        VEC1(I)=70.0
2      CONTINUE

```

VEC(1)=TSTEAM\*(AX\*DELT/DELX\*\*2.+ MF\*CF\*DELT/DELX)/CONST

```

* + TSTEAM
DO 200 P=1,10
PDT=P*DELT

C
C
C      I=1

      B(1)=((1-VF)*ROS*CS + (2*AX*DELT)/DELX**2 + MF*CF*DELT
*      /DELX)/CONST
      C(1)=(-AX*DELT/DELX**2)/CONST

C
C
C      I=2, NNOD-1

DO 20 I=2, NNOD-1
      B(I)=((1-VF)*ROS*CS + (2*AX*DELT)/DELX**2 + MF*CF*DELT
*      /DELX)/CONST
      A(I)=(-AX*DELT/DELX**2 - MF*CF*DELT/DELX)/CONST
      C(I)=(-AX*DELT/DELX**2)/CONST
20    CONTINUE

C
C
C      I=NNOD

      B(NNOD)=((1-VF)*ROS*CS + AX*DELT/DELX**2 + MF*CF*DELT
*      /DELX)/CONST
      A(NNOD)=(-AX*DELT/DELX**2 - MF*CF*DELT/DELX)/CONST

      CALL TRIDAG (1, NNOD, A, B, C, VEC, T)

      VEC(1)=TSTEAM+TSTEAM*(AX*DELT/DELX**2 + MF*CF*DELT/DELX
*      )/CONST

40    DO 40 I=2, NNOD
      VEC(I)=T(I)

C
C
C      CLOTH CALCULATIONS
      NODE 1, I=NNOD+1

      B1(1)=((1-VFC)*ROC*CC + (2*AXC*DELT)/DELXC**2 + MF*CF*DELT
*      /DELXC)/CONSTC
      C1(1)=(-AXC*DELT/DELXC**2)/CONSTC

C
C
C      I=NNOD+2, NNODC-1

DO 51 I=2, NNODC-1
      B1(I)=((1-VFC)*ROC*CC + (2*AXC*DELT)/DELXC**2 + MF*CF*DELT
*      /DELXC)/CONSTC
      C1(I)=(-AXC*DELT/DELXC**2)/CONSTC
      A1(I)=(-AXC*DELT/DELXC**2 - MF*CF*DELT/DELXC)/CONSTC
51    CONTINUE

C
C
C      I=NNODC

      B1(NNODC)=((1-VFC)*ROC*CC + AXC*DELT/DELXC**2 + MF*CF*DELT
*      /DELXC)/CONSTC
      A1(NNODC)=(-AXC*DELT/DELXC**2 - MF*CF*DELT/DELXC)/CONSTC

      VEC1(1)=T(NNOD)*(AXC*DELT/DELXC**2 + MF*CF*DELT/DELXC)

```

```

C
C      I=NNOD+2,NNODC-1
C
      DO 51 I=2,NNODC-1
      B1(I)=((1-VFC)*ROC*CC + (2*AXC*DELT)/DELXC**2 + MF*CF*DELT
*      /DELXC)/CONSTC
      C1(I)=(-AXC*DELT/DELXC**2)/CONSTC
      A1(I)=(-AXC*DELT/DELXC**2 -MF*CF*DELT/DELXC)/CONSTC
51      CONTINUE

C
C      I=NNODC
C
      B1(NNODC)=((1-VFC)*ROC*CC + AXC*DELT/DELXC**2 + MF*CF*DELT
*      /DELXC)/CONSTC
      A1(NNODC)=(-AXC*DELT/DELXC**2 - MF*CF*DELT/DELXC)/CONSTC

      VEC1(1)=T(NNOD)*(AXC*DELT/DELXC**2 +MF*CF*DELT/DELXC)
*      /CONSTC + T(NNOD)

      CALL TRIDAG(1,NNODC,A1,B1,C1,VEC1,T1)

      VEC1(1)=T(NNOD)+T(NNOD)*(AXC*DELT/DELXC**2 + MF*CF*DELT
*      /DELXC)/CONSTC
      DO 41 I=2,NNODC
41      VEC1(I)=T1(I)

      WRITE (5,23) PDT
23      FORMAT(/,'TIME = ',F5.1,' SECS')

      WRITE (5,160)
160      FORMAT (/,'NODAL TEMPERATURES FOR SINTERED MATERIAL ...')
      DO 175 I=1,NNOD
      IP1=NNOD + I
      WRITE (5,150) I,T(I)
150      FORMAT('T(',I2,') = ',F10.3)
175      CONTINUE

      WRITE (5,161)
161      FORMAT (/,'NODAL TEMPERATURES FOR CLOTH ...')
      DO 176 I=1,NNODC
      IP1=NNOD + I
      WRITE (5,151) IP1,T1(I)
151      FORMAT('T(',I2,') = ',F10.3)
176      CONTINUE

200      CONTINUE

      END

C
C      SUBROUTINE TRIDAG SOLVES A DIAGONAL SYSTEM OF EQUATIONS.
C      A(N), B(N), C(N) ARE SUB-DIAGONAL, DIAGONAL, AND SUPER-
C      DIAGONAL TERMS, RESPECTIVELY.

      SUBROUTINE TRIDAG(IF,L,A,B,C,D,V)
      DIMENSION A(1),B(1),C(1),D(1),V(1),BETA(101),GAMMA(101)
      BETA(IF) = B(IF)
      GAMMA(IF) = D(IF)/BETA(IF)
      IFP1=IF+1
      DO 1 I=IFP1,L
      BETA(I)=B(I)-A(I)*C(I-1)/BETA(I-1)
1      GAMMA(I)=(D(I)-A(I)*GAMMA(I-1))/BETA(I)

      V(L)=GAMMA(L)

```

```
2      LAST=L-IF  
        DO 2 K=1, LAST  
          I=L-K  
          V(I)=GAMMA(I)-C(1)*V(I+1)/BETA(I)  
        RETURN  
      END
```

```

C THIS PROGRAM USES THE IMPLICIT FINITE DIFFERENCE METHOD
C OUTLINED IN INCROPERA & DEWITT, FUNDAMENTALS OF HEAT AND
C MASS TRANSFER, SECOND EDITION, TO DETERMINE THE TEMPERATURE
C DISTRIBUTION WITHIN CLEMSON UNIVERSITY'S DESIGN OF A COLLAR
C BAND FOLDING DEVICE. 1-D EXPRESSIONS ARE USED, AND HEAT
C TRANSFER RELATIONS ARE USED FOR SOLID POROUS MEDIA ACCORDING
C TO D. VORTMEYER AND R. J. SCHAEFER, EQUIVALENCE OF ONE- AND
C TWO-PHASE MODELS FOR HEAT TRANSFER PROCESSES IN PACKED BEDS:
C ONE DIMENSIONAL THEORY, CHEMICAL ENGINEERING SCIENCE, 1974,
C VOL. 29, PP. 485-491.

```

```

      DIMENSION A2(50),B2(50),C2(50),T2(50),VEC2(50)
      REAL KSL
      INTEGER P
      OPEN (unit = 5,file = 'lpt1')
      DELT=0.001
      KSL=.0024
      NNODSL=20
      ROSL=485.
      CSL=0.114
      MF=0.001389
      CF=0.47
      HFC=0.00087
      HSL=0.7
      XLENL=.125/12.
      DELXSL=XLENL/(NNODSL-1)
      ALPHA=KSL/(ROSL*CSL)
      TAIR=70.
      TSTEAM=415.

```

```

C
C      INITIALIZE MATRICES
C

```

```

      DO 3 I=1,NNODSL
      A2(I)=0.0
      B2(I)=0.0
      C2(I)=0.0
      VEC2(I)=70.0
      T2(I)=70.0
3      CONTINUE

```

```

      DO 200 P=1,50
      PDT=P*DELT

```

```

C
C      STEEL CALCULATIONS
C      I=1
C

```

```

      C2(1)=-2.*ALPHA*DELT/DELXSL**2.
      B2(1)=1.+(2.*ALPHA*DELT)/DELXSL**2. + 2.*HSL*DELT/
      * (ROSL*CSL*DELXSL)

```

```

C
C      I=2,NNODSL-1
C

```

```

      DO 60 I=2,NNODSL-1
      A2(I)=-2.*ALPHA*DELT/DELXSL**2.
      B2(I)=(2.*ALPHA*DELT)/DELXSL**2. + 1.
      C2(I)=-ALPHA*DELT/DELXSL**2.
60      CONTINUE

```

```

C
C      I=NNODSL
C

```

```

      A2(NNODSL)=-2.*ALPHA*DELT/DELXSL**2.
      B2(NNODSL)=1.+(2.*ALPHA*DELT)/DELXSL**2.+2.*HFC*DELT/
      * (ROSL*CSL*DELXSL)

```

```

      VEC2(1) = T2(1) + (2.*HSL*DELT/(ROSL*CSL*DELXSL))*TSTEAM
      VEC2(NNODSL)=T2(NNODSL) + (2*HFC*DELT/(ROSL*CSL*DELXSL)
*      )*TAIR

      CALL TRIDAG(1,NNODSL,A2,B2,C2,VEC2,T2)

      VEC2(1) = T2(1) + (2.*HSL*DELT/(ROSL*CSL*DELXSL))*TSTEAM
      VEC2(NNODSL)=T2(NNODSL) + (2*HFC*DELT/(ROSL*CSL*DELXSL)
*      )*TAIR

      DO 42 I=2,NNODSL-1
42      VEC2(I)=T2(I)

      WRITE (5,23) PDT
23      FORMAT(/,'TIME = ',F10.7,' SECS')

      WRITE (5,162)
162      FORMAT (/,'NODAL TEMPERATURES FOR BLADES ...')
      DO 177 I=1,NNODSL
      WRITE(5,152) I,T2(I)
152      FORMAT('T(',I2,') = ',F10.3)
177      CONTINUE

200      CONTINUE

      END

C
C      SUBROUTINE TRIDAG SOLVES A DIAGONAL SYSTEM OF EQUATIONS.
C      A(N), B(N), C(N) ARE SUB-DIAGONAL, DIAGONAL, AND SUPER-
C      DIAGONAL TERMS, RESPECTIVELY.

      SUBROUTINE TRIDAG(IF,L,A,B,C,D,V)
      DIMENSION A(1),B(1),C(1),D(1),V(1),BETA(101),GAMMA(101)
      BETA(IF) = B(IF)
      GAMMA(IF) = D(IF)/BETA(IF)
      IFP1=IF+1
      DO 1 I=IFP1,L
      BETA(I)=B(I)-A(I)*C(I-1)/BETA(I-1)
1      GAMMA(I)=(D(I)-A(I)*GAMMA(I-1))/BETA(I)

      V(L)=GAMMA(L)
      LAST=L-IF
      DO 2 K=1,LAST
      I=L-K
2      V(I)=GAMMA(I)-C(1)*V(I+1)/BETA(I)
      RETURN
      END

```

Appendix EOutput from Finite-Difference Models



TIME = 0.1 SECS

NODAL TEMPERATURES FOR SINTERED MATERIAL ...

T( 1) = 338.858  
T( 2) = 247.719  
T( 3) = 191.548  
T( 4) = 159.294  
T( 5) = 144.611

NODAL TEMPERATURES FOR CLOTH ...

T( 6) = 127.284  
T( 7) = 95.638  
T( 8) = 81.581  
T( 9) = 75.484  
T(10) = 73.191

TIME = 0.2 SECS

NODAL TEMPERATURES FOR SINTERED MATERIAL ...

T( 1) = 367.401  
T( 2) = 310.427  
T( 3) = 265.787  
T( 4) = 235.754  
T( 5) = 220.767

NODAL TEMPERATURES FOR CLOTH ...

T( 6) = 190.070  
T( 7) = 134.005  
T( 8) = 103.715  
T( 9) = 88.425  
T(10) = 82.056

TIME = 0.3 SECS

NODAL TEMPERATURES FOR SINTERED MATERIAL ...

T( 1) = 382.971  
T( 2) = 344.635  
T( 3) = 313.026  
T( 4) = 290.711  
T( 5) = 279.209

NODAL TEMPERATURES FOR CLOTH ...

T( 6) = 241.853  
T( 7) = 173.626  
T( 8) = 131.369  
T( 9) = 107.573  
T(10) = 96.905

TIME = 0.4 SECS

NODAL TEMPERATURES FOR SINTERED MATERIAL ...

T( 1) = 393.020  
T( 2) = 366.711  
T( 3) = 344.743  
T( 4) = 329.016  
T( 5) = 320.826

NODAL TEMPERATURES FOR CLOTH ...

T( 6) = 281.448  
T( 7) = 209.527  
T( 8) = 160.504  
T( 9) = 130.650  
T(10) = 116.541

TIME = 0.5 SECS

NODAL TEMPERATURES FOR SINTERED MATERIAL ...

T( 1) = 399.836  
T( 2) = 381.685  
T( 3) = 366.478  
T( 4) = 355.548  
T( 5) = 349.838

NODAL TEMPERATURES FOR CLOTH ...

T( 6) = 311.115  
T( 7) = 240.391  
T( 8) = 188.792  
T( 9) = 155.553  
T(10) = 139.243

TIME = 0.6 SECS

NODAL TEMPERATURES FOR SINTERED MATERIAL ...

T( 1) = 404.523  
T( 2) = 391.982  
T( 3) = 381.466  
T( 4) = 373.898  
T( 5) = 369.942

NODAL TEMPERATURES FOR CLOTH ...

T( 6) = 333.303  
T( 7) = 266.385  
T( 8) = 215.112  
T( 9) = 180.717  
T(10) = 163.377

TIME = 0.7 SECS

NODAL TEMPERATURES FOR SINTERED MATERIAL ...

T( 1) = 407.758  
T( 2) = 399.090  
T( 3) = 391.819  
T( 4) = 386.586  
T( 5) = 383.849

NODAL TEMPERATURES FOR CLOTH ...

T( 6) = 349.988  
T( 7) = 288.144  
T( 8) = 239.032  
T( 9) = 205.100  
T(10) = 187.657

TIME = 0.8 SECS

NODAL TEMPERATURES FOR SINTERED MATERIAL ...

T( 1) = 409.994  
T( 2) = 404.002  
T( 3) = 398.976  
T( 4) = 395.357  
T( 5) = 393.465

NODAL TEMPERATURES FOR CLOTH ...

T( 6) = 362.651  
T( 7) = 306.372  
T( 8) = 260.476  
T( 9) = 228.072  
T(10) = 211.175

TIME = 0.9 SECS

NODAL TEMPERATURES FOR SINTERED MATERIAL ...

T( 1) = 411.539  
T( 2) = 407.397  
T( 3) = 403.922  
T( 4) = 401.421  
T( 5) = 400.113

NODAL TEMPERATURES FOR CLOTH ...

T( 6) = 372.368  
T( 7) = 321.695  
T( 8) = 279.541

T( 9) = 249.296  
T(10) = 233.358

TIME = 1.0 SECS

NODAL TEMPERATURES FOR SINTERED MATERIAL ...

T( 1) = 412.608  
T( 2) = 409.744  
T( 3) = 407.342  
T( 4) = 405.613  
T( 5) = 404.708

NODAL TEMPERATURES FOR CLOTH ...

T( 6) = 379.917  
T( 7) = 334.638  
T( 8) = 296.399  
T( 9) = 268.631  
T(10) = 253.884

TIME = 0.0010000 SECS

NODAL TEMPERATURES FOR BLADES ...

T( 1) =	87.344
T( 2) =	94.997
T( 3) =	94.198
T( 4) =	94.072
T( 5) =	94.045
T( 6) =	94.039
T( 7) =	94.037
T( 8) =	94.037
T( 9) =	94.037
T(10) =	94.037
T(11) =	94.037
T(12) =	94.037
T(13) =	94.036
T(14) =	94.034
T(15) =	94.023
T(16) =	93.976
T(17) =	93.774
T(18) =	92.892
T(19) =	89.061
T(20) =	72.405

TIME = 0.0020000 SECS

NODAL TEMPERATURES FOR BLADES ...

T( 1) =	107.043
T( 2) =	126.002
T( 3) =	126.308
T( 4) =	126.351
T( 5) =	126.340
T( 6) =	126.332
T( 7) =	126.329
T( 8) =	126.328
T( 9) =	126.328
T(10) =	126.328
T(11) =	126.327
T(12) =	126.326
T(13) =	126.322
T(14) =	126.304
T(15) =	126.239
T(16) =	125.992
T(17) =	125.088
T(18) =	121.902
T(19) =	111.274
T(20) =	79.077

TIME = 0.0030000 SECS

NODAL TEMPERATURES FOR BLADES ...

T( 1) =	130.167
T( 2) =	164.682
T( 3) =	168.432
T( 4) =	169.431
T( 5) =	169.654
T( 6) =	169.698
T( 7) =	169.706
T( 8) =	169.707
T( 9) =	169.706
T(10) =	169.706
T(11) =	169.704
T(12) =	169.699
T(13) =	169.679
T(14) =	169.611
T(15) =	169.377
T(16) =	168.601
T(17) =	166.138
T(18) =	158.769
T(19) =	138.534
T(20) =	90.079

TIME = 0.0040000 SECS

NODAL TEMPERATURES FOR BLADES ...

T( 1) =	157.995
T( 2) =	213.244
T( 3) =	223.382
T( 4) =	226.690
T( 5) =	227.640
T( 6) =	227.896
T( 7) =	227.961
T( 8) =	227.976
T( 9) =	227.979
T(10) =	227.978
T(11) =	227.973
T(12) =	227.954
T(13) =	227.890
T(14) =	227.686
T(15) =	227.051
T(16) =	225.163
T(17) =	219.842
T(18) =	205.898
T(19) =	172.909
T(20) =	105.910

TIME = 0.0050000 SECS

NODAL TEMPERATURES FOR BLADES ...

T( 1) =	192.111
T( 2) =	274.591
T( 3) =	294.878
T( 4) =	302.547
T( 5) =	305.122
T( 6) =	305.931
T( 7) =	306.172
T( 8) =	306.240
T( 9) =	306.257
T(10) =	306.256
T(11) =	306.240
T(12) =	306.184
T(13) =	306.013
T(14) =	305.504
T(15) =	304.052
T(16) =	300.114
T(17) =	290.076
T(18) =	266.493
T(19) =	216.861
T(20) =	127.486

TIME = 0.0060000 SECS

NODAL TEMPERATURES FOR BLADES ...

T( 1) =	234.528
T( 2) =	352.527
T( 3) =	387.833
T( 4) =	402.811
T( 5) =	408.473
T( 6) =	410.466
T( 7) =	411.130
T( 8) =	411.339
T( 9) =	411.399
T(10) =	411.402
T(11) =	411.360
T(12) =	411.220
T(13) =	410.815
T(14) =	409.694
T(15) =	406.731
T(16) =	399.317
T(17) =	381.976
T(18) =	344.774
T(19) =	273.477
T(20) =	156.174

Appendix F  
System Thermodynamic Considerations  
for Clemson Device

In order to gain some understanding of the operating power required for the superheater, consider a worst case scenario. Since the folder was open to the atmosphere, it was obvious that the folding system operated at pressures near atmospheric pressure. From information obtained during the operation of the folding mechanism, a worst case scenario could be estimated by considering a pressure drop of 3 psi from the steam generator to some point slightly downstream of the superheater. Let the generator pressure ( $P_1$ ) equal 18 psia and the pressure downstream of the superheater ( $P_2$ ) equal 15 psia. Also, the desired temperature downstream of the superheater was the temperature defined by the folding parameters. Hence, the temperature downstream of the superheater ( $T_2$ ) was 450°F maximum.

The steam state upstream of the superheater, however, was not so clearly defined. At best, the steam was saturated coming from the boiler. However, with heat losses from the pipe and pressure differentials through the pipe, the quality of the steam was assuredly less than 1.0. Pressure drop could not be calculated analytically across the superheater, so completely defining the steam state upstream was impossible without empirical data. However, since the folder was open to the atmosphere,  $P_1$  was estimated to operate near or slightly above  $P_{atm}$ .

The maximum value for the quality of the steam ( $x$ ) at the exit of the steam generator was 1.0, signifying completely saturated steam. As an estimate of the actual steam quality, consider  $x = 0.9$  for 90% saturated steam. Since the quality of the steam was less than 1.0, a change of state of the additional liquid water must occur in the superheater.

For a partial change of state in the superheater, the First Law of Thermodynamics could be written as:

$$Q_{in} = m(h_{out} - h_{in})$$

for the steady state, steady flow superheater where

$Q_{in}$  is the power requirement of the superheater

$m$  is the mass flow rate

$h_{out}$  is the exit enthalpy

$h_{in}$  is the entrance enthalpy.

Upon entrance to the superheater, the enthalpy of the steam for a change of state within the superheater was calculated as:

$$h_{in} = h_l + (x)h_{lg}$$

where  $h_l$  is the enthalpy of the liquid state

$h_{lg}$  is the enthalpy of transition from liquid to vapor

$x$  is the steam quality.

From tabulated steam tables,

$h_{out} = 1255$  Btu/lbm for superheated steam at 450° F and 15 psi

$h_l = 190$  Btu/lbm for liquid water at 212° F

$h_{lg} = 962$  Btu/lbm for phase transition of water at 212° F.

The mass flow rate at the maximum capacity of the generator is 5 lbm/hr. Therefore, the expected power requirement for operating the superheater is 845 Btu/hr or



about 250 W. This expected power requirement is well within the operating range of the superheater.

## Appendix G

### Error Factors in Temperature Readings

Errors in thermocouple measurements come from uncertainty in knowing the temperature of the thermocouple probe and from physical errors in accounting for heat losses in probe insertion. Figure G-1 depicts the three primary physical mechanisms which may cause the thermocouple to give erroneous information[5]: (1) conduction, (2) radiation, and (3) velocity errors (also termed recovery errors). Consider the temperature probe in an internal flow as shown in Figure G-1. The thermocouple bead and the leads form the path for energy conduction. Conduction along the thermocouple leads away from the thermocouple bead can be modeled as a one-dimensional fin. For a differential element of the fin at steady state, there is energy conducted along the fin, and transferred by convection from the surface. The surface area for convection is  $Pdx$ , where  $P$  is the circumference, and  $dx$  is the differential length of the fin. By applying the First Law of Thermodynamics to the differential element, the following energy balance is obtained:

$$Q_x + dQ_x - Q_{x+dx} = hPdx (T(x) - T_\infty)$$

where  $h$  is the convective heat transfer coefficient  
 $T(x)$  is the temperature of the fin at some  
distance  $x$  from the origin  
 $T_\infty$  is the temperature of the flow (steam).

Expanding  $Q$  in a Taylor series expansion about the point  $x$ , and substituting  $\theta$  for  $(T - T_\infty)$  and  $-k(dT/dx)$  for  $Q$ , where

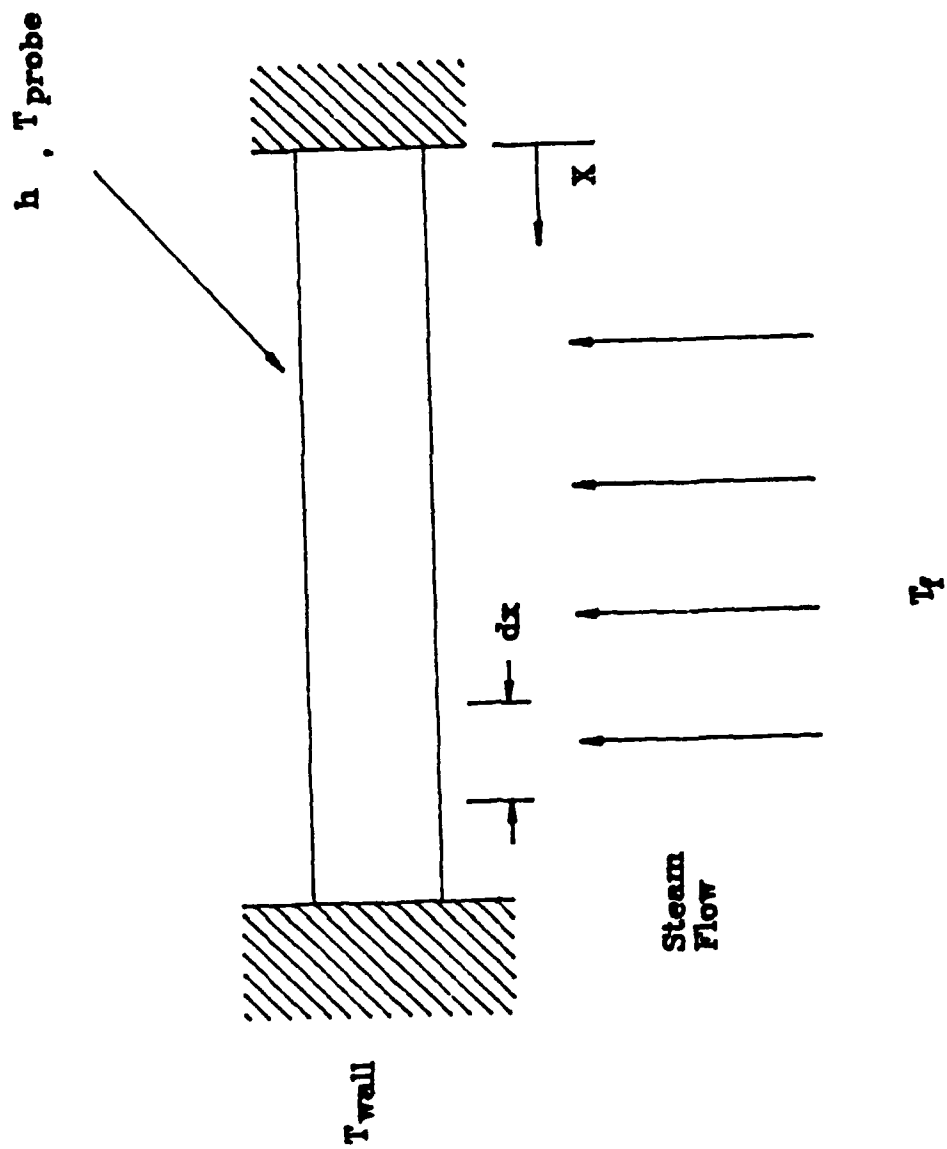


Figure G-1. Thermocouple Approximation

$k$  is the effective thermal conductivity of the probe, then the governing differential equation is:

$$d^2\theta/dx^2 - M^2\theta = 0.$$

$M$  is equal to  $(hP/kA)^{1/2}$  and  $A$  is the surface area of the bead. The boundary conditions for solving this differential equation are that the wall has a temperature  $T_w$ , or a normalized value  $\theta_w = T_w - T_\infty$ , and that the surface area of the end of the fin is small. The solution, therefore, is[5]:

$$\theta(x)/\theta_w = \cosh(Mx)/\cosh(ML)$$

where  $L$  is the length of probe insertion into the flow. The point  $x = 0.0$  is assumed to be the tip of the fin where the temperature is being measured. Hence,

$$\theta(0)/\theta_w = 1/\cosh(ML)$$

The goal of the probe design is to maximize the term  $ML$  since the hyperbolic cosine function increases with increasing  $ML$ , thus reducing the error. Therefore, the thermocouple bead should be as small in diameter as possible, and the length of insertion should be as large as possible.

In order to evaluate the conduction error, the system parameters are established as follows (see Figure G-2):

$D$  = flow diameter  
 $V$  = flow velocity  
 $\rho$  = flow density  
 $\nu$  = flow viscosity  
 $m$  = mass flow rate of steam  
 $A$  = flow area  
 $Re$  = Reynolds number based on diameter  $D$ ;  $Re = VD/\nu$   
 $Nu$  = Nusselt number or non-dimensionalized convective coefficient;  $Nu = hD/k = 0.44 Re^{0.5}$  for leads perpendicular to flow.

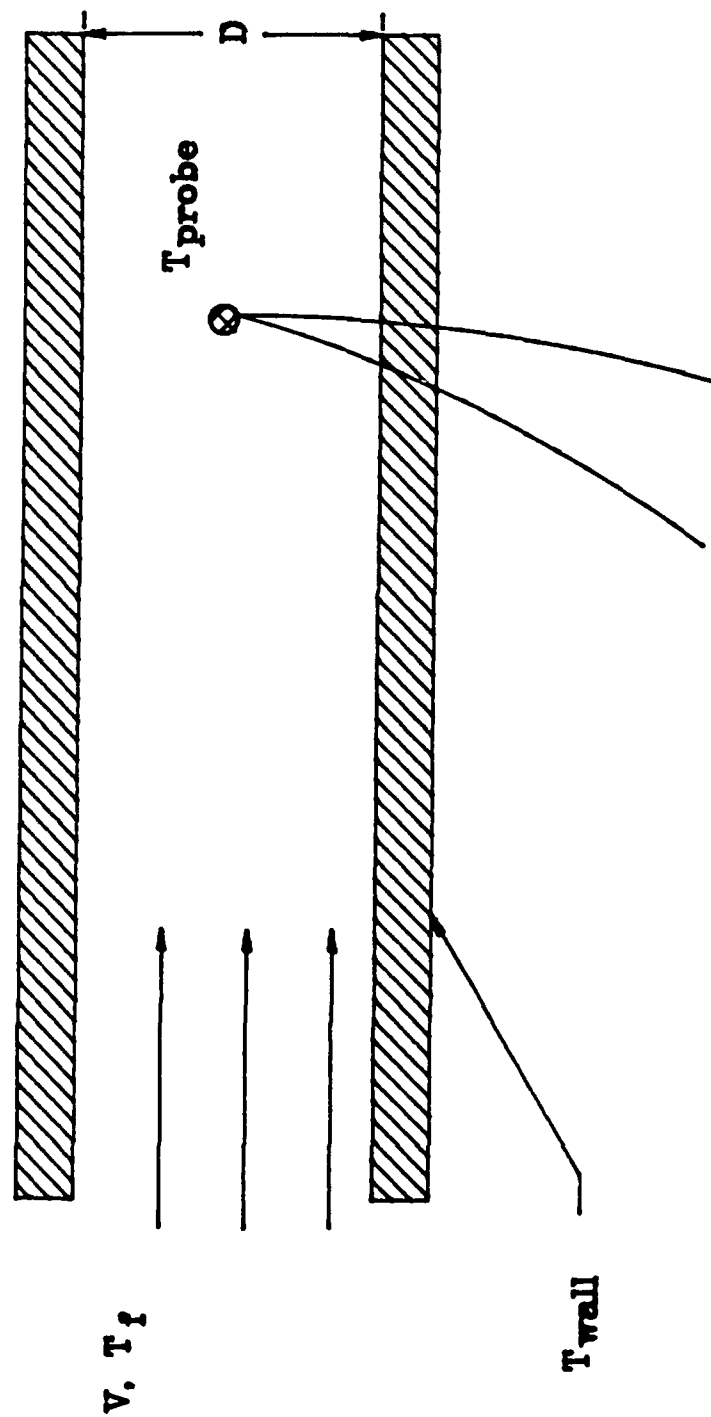


Figure G-2. System Parameters - Fin Approximation

The conduction error is of the form[5]:

$$E_C = (T_W - T_\infty) / \cosh[(hP/kA)^{1/2}L].$$

For the folding unit, error in conduction varied directly with the temperature difference  $(T_W - T_\infty)$ . From empirical data taken during the experiment, the order of the temperature difference was nominally about 3° F. Therefore, the errors induced by conduction in the thermocouple were estimated as less than 1% of the total temperature reading.

The radiation error and the recovery error both proved to be negligible due to small temperature differences and low flow rates. The major component of the thermocouple error is that caused by conduction.

## Appendix H

### Uncertainty Analysis in Measured Quantities

In reporting empirical data from the experimental setups, the results must be reported with some confidence level, i. e. some effort has to be made to quantify how much error there may be included in the data.

The particular type of uncertainty analysis which was used with this experiment was a design stage uncertainty analysis. Sources of uncertainty were obtained from reported figures from the manufacturer of the equipment used, and from resolution errors introduced in taking the data from the read-out or gauge accompanying the measuring instrument. Table H.I lists by source the errors which were present in temperature, pressure, and moisture measurements. The uncertainty for each measurement was encountered from manufacturer's specifications, which were included in the instrument literature, and from resolution errors which were those errors introduced by the gauge or "readout mechanism" accompanying the measuring instrument.

As can be noted in Table H.I, each source of uncertainty in a particular measurement can be combined to obtain an overall, or total, uncertainty associated with each measurement. Each uncertainty associated with a particular measurement can be combined to find this total uncertainty using one form of the Kline-McClintock Theory. For example,

the uncertainty in the temperature measurement can be found as follows[5]:

Table H-I. Uncertainties in Measured Quantities

Entity	Uncertainty Source	Uncertainty Type	Amount of Uncertainty	Total Uncertainty
Temperature	Thermocouple	Manuf. Spec.	2.5°F	
	Digital Readout	Manuf. Spec.	1.0°F	
	Digital Readout	Resolution	0.5°F	2.75°F
Pressure	Bourdon Tube	Manuf. Spec.	2 psi	
	Bourdon Tube	Resolution	0.5 psi	2.1 psi
Moisture	Textometer	Manuf. Spec.	0.2%	
	Textometer	Resolution	0.1%	0.22%

$$(U_T) = [U_1^2 + U_2^2 + U_3^2]^{1/2}$$

where  $U_T$  = total uncertainty in temperature

$U_1$  = uncertainty in thermocouple wire



$U_2$  = uncertainty in digital readout

$U_3$  = uncertainty in resolution of digital  
readout.

### Temperature Measurements

The objective of temperature measurement in the Clemson device was to more fully establish temperatures required to fold cloth. Temperature measurements at strategic locations in the manifold section of the machine provided data for evaluating the validity of the heat transfer models. Temperature measurements of the manifold at various places along the flow path provided empirical data for estimating heat transfer to and from the manifold. Steam temperatures were monitored in the flow stream using a sheathed thermocouple. As presented in Appendix G, errors incurred in the temperature measurements were primarily due to losses through conduction. These losses were estimated at less than 1% of the total temperature measurement.

As a result, temperature data taken empirically could be reported at some fixed amount, plus or minus some uncertainty, say  $275^{\circ}\text{F} \pm 2.75^{\circ}\text{F}$ . Then, there is relative certainty that the true value of the reported temperature lies between  $272.25$  and  $277.75^{\circ}\text{F}$ . A similar analysis can be conducted with the pressure and moisture data, also.

Appendix ITabulated Experimental Results - Clemson Device





	55% Polyester				45% Cotton				Pressure (psi)				D1				D2				Θ <sub>1</sub>				Θ <sub>2</sub>			
	Steam Temp (F)	Ins Wall Temp (F)	Out Wall Temp (F)	Bronze Temp (F)	Dry Time (Cotton)	Heat Time (Poly)	Cool Time (Poly)	Cycle Time (s)					dm1	dm2	dm1	dm2	dm1	dm2	dm1	dm2	dm1	dm2	dm1	dm2	dm1	dm2	dm1	dm2
1.	320	319	317	320	25	25	11	36	27	27	27	27	.282	.281	.282	.283	.379	.361	.379	.361	42°	42°	42°	42°	39°	39°	39°	39°
2.	325	324	322	324	26	27	11	38	27	27	27	27	.216	.217	.216	.217	.284	.284	.284	.284	41°	41°	41°	41°	35°	35°	35°	35°
3.	330	330	329	330	24	27	12	39	24	24	24	24	.294	.294	.294	.294	.315	.315	.315	.315	21°	21°	21°	21°	20°	20°	20°	20°
4.	335	332	331	333	21	25	14	39	25	25	25	25	.287	.287	.287	.287	.304	.304	.304	.304	19°	19°	19°	19°	17°	17°	17°	17°
5.	340	337	334	337	20	25	15	40	26	26	26	26	.279	.279	.279	.279	.288	.288	.288	.288	14°	14°	14°	14°	17°	17°	17°	17°
6.	345	342	342	343	20	25	17	42	24	24	24	24	.291	.291	.291	.291	.297	.297	.297	.297	13°	13°	13°	13°	12°	12°	12°	12°
7.	350	348	347	348	19	24	19	43	25	25	25	25	.319	.319	.319	.319	.321	.321	.321	.321	6°	6°	6°	6°	7°	7°	7°	7°
8.	355	355	355	355	17	21	20	41	25	25	25	25	FLAT	FLAT	FLAT	FLAT	FLAT	FLAT	FLAT	FLAT								
9.	360	360	358	359	15	20	21	41	26	26	26	26	FLAT	FLAT	FLAT	FLAT	FLAT	FLAT	FLAT	FLAT								

Sample Data Listing for Clemson Device





100% cotton	Steam Temp (F)	Ins Wall Temp (F)	Dut Wall Temp (F)	Bronze Temp (F)	Dry Time (Cotton)	Heat Time (Poly)	Cool Time (Poly)	Cycle Time (s)	Pressure (psi)	D1		D2		D1		D2	
										dm1	θ <sub>1</sub>	dm2	θ <sub>2</sub>	dm1	θ <sub>1</sub>	dm2	θ <sub>2</sub>
	300	300	297	298	66			66	24	.297 NC	38° NC	.326 NC	.418 NC	.297 NC	38° NC	.326 NC	.418 NC
	305	304	301	304	62			62	24	.281 NC	29° NC	.301 NC	.335 NC	.281 NC	29° NC	.301 NC	.335 NC
	310	308	304	310	60			60	25	.280 NC	12° NC	.300 NC	.310 NC	.280 NC	12° NC	.300 NC	.310 NC
	315	312	311	314	56			56	26	.274 NC	8° NC	.330 NC	.331 NC	.274 NC	8° NC	.330 NC	.331 NC
	320	318	316	319	47			47	25	FLAT				FLAT			
	325	324	323	325	42			42	25	FLAT				FLAT			
	330	330	328	330	36			36	25	FLAT				FLAT			
	335	334	331	337	30			30	26	FLAT				FLAT			
	340	339	338	338	28			28	24	FLAT				FLAT			

Sample Data Listing for Clemson Device



## Moisture Content for 70/30 Poly/Cotton

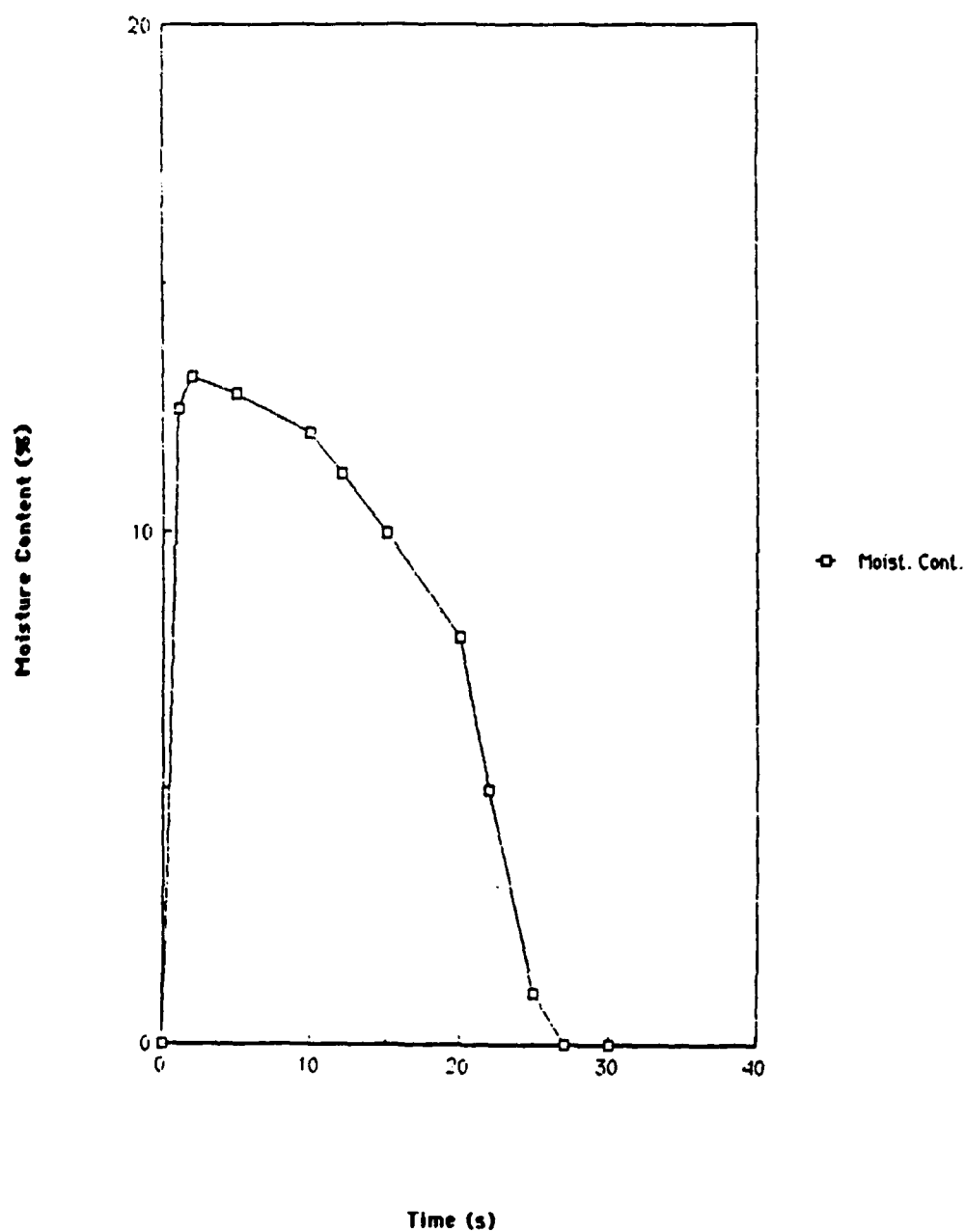


Figure I-1. Moisture Content vs. Time for 70/30 Polyester/Cotton Blend

## Moisture Content vs. Time for 55/45 Poly/Cotton

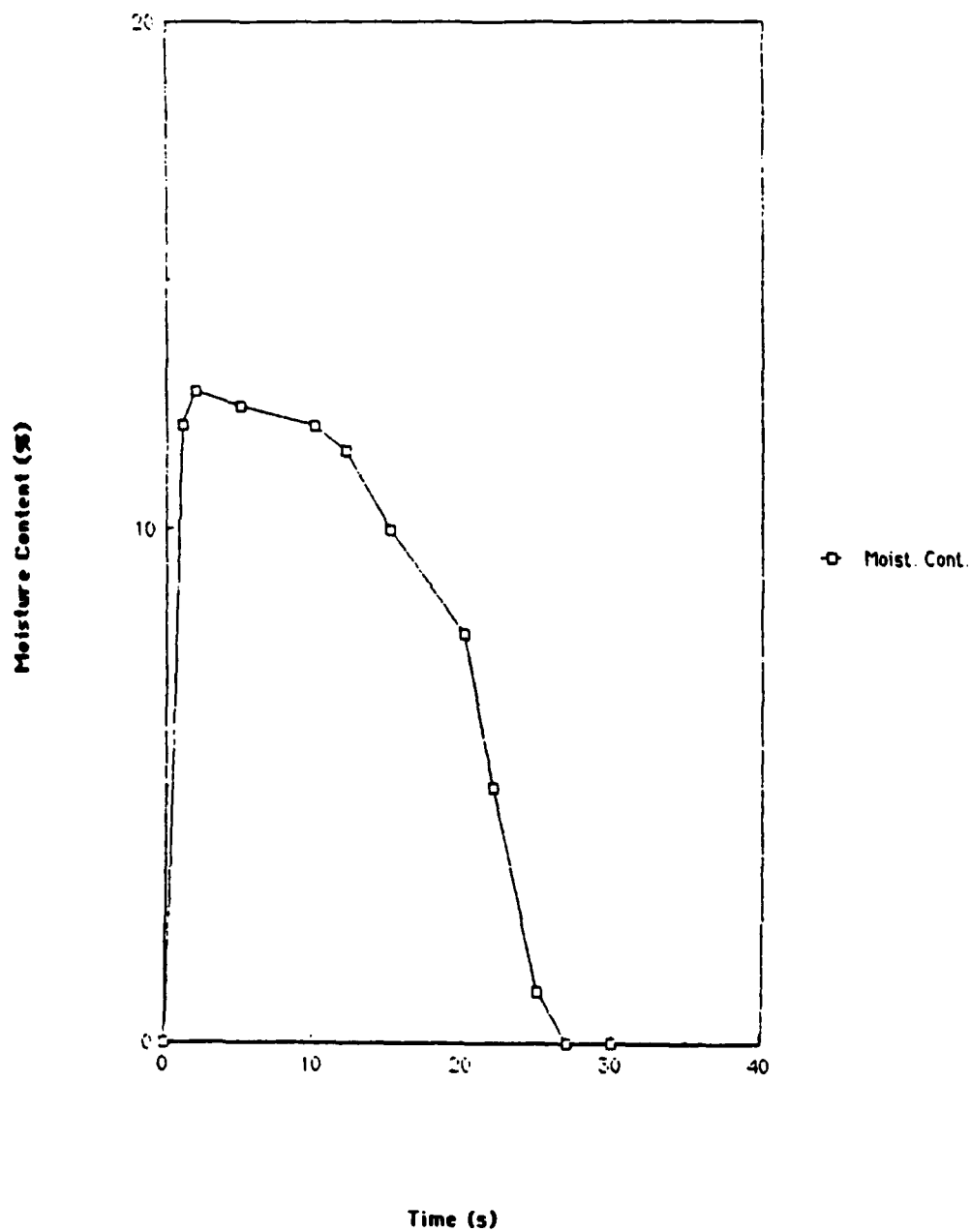


Figure I-2. Moisture Content vs. Time for 55/45 Polyester/Cotton Blend

## Moisture Content vs. Time for 65/35 Cotton/Poly

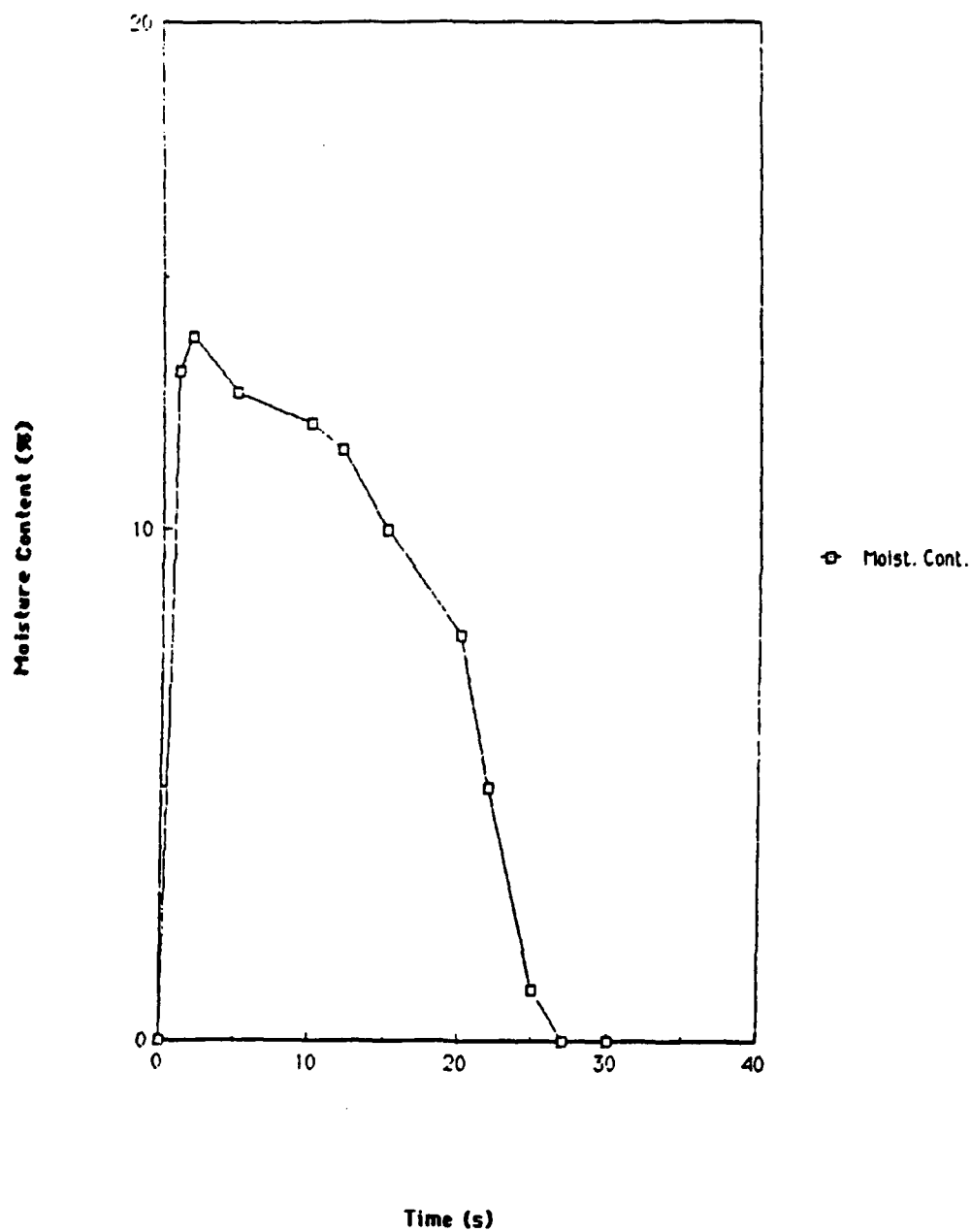


Figure I-3. Moisture Content vs. Time for 65/35 Cotton/Polyester Blend

## Moisture Content vs. Time for 100% Cotton

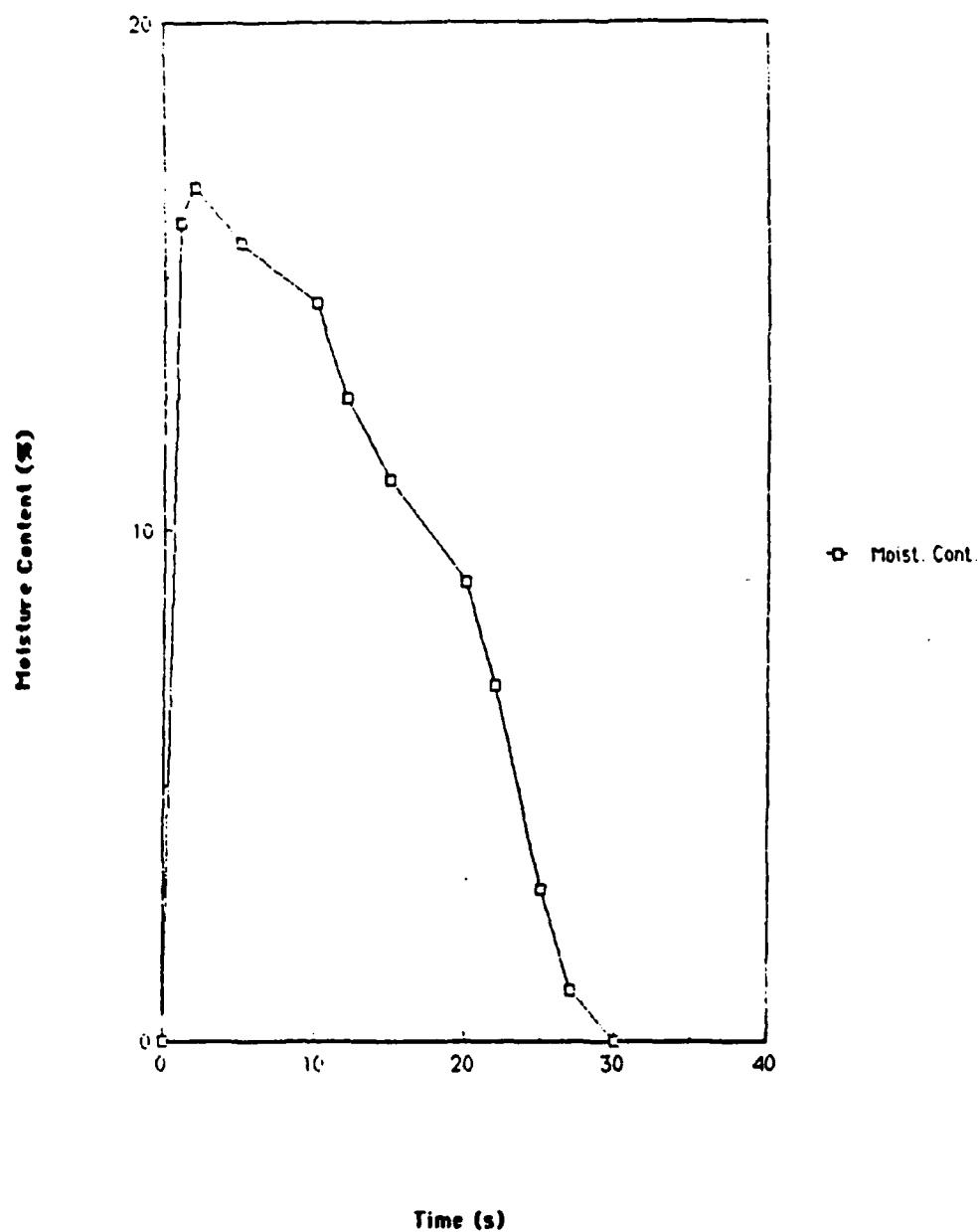


Figure I-4. Moisture Content vs. Time for 100% Cotton Fabric

Appendix JTabulated Experimental Results - Jet Sew Device



DATA SET 2:  
70/30  
POLYESTER/COTTON

	Heat Temp (F)	Cavity Temp (F)	Heat Time (s)	Pressure (psi)	Cool Temp (F)	Cavity Temp (F)	Cool Time (s)	Cycle Time (s)	dm1	D1	Q1	dm2	D2	Q2
1.	450	200	12	20	68	150	8	20	.273 .273 .255 .255	.276 .276 .257 .25	8 8 8 8	.239 .239 .243 .243	.241 .241 .245 .245	7 7 8 8
2.	450	205	15	20	68	150	15	30	.281 .281 .283 .283	.283 .283 .283 .283	7 7 7 7	.219 .219 .219 .219	.220 .220 .220 .220	7 7 7 7
3.	450	210	15	20	67	130	25	40	.375 .375 .375 .375	.380 .380 .380 .380	10 10 10 10	.225 .225 .225 .225	.233 .233 .233 .233	15 15 15 15
4.	450	210	14	20	70	150	6	20	.300 .300 .300 .300	.305 .305 .305 .305	10 10 10 10	.413 .413 .413 .413	.419 .419 .419 .419	10 10 10 10
5.	450	215	21	20	69	150	8	29	.313 .313 .313 .313	.314 .314 .314 .314	5 5 5 5	.187 .187 .187 .187	.188 .188 .188 .188	5 5 5 5
6.	450	220	25	20	68	130	35	60	.375 .375 .375 .375	.375 .375 .375 .375	0 0 0 0	.350 .350 .350 .350	.350 .350 .350 .350	0 0 0 0
7. FLAT FOLD	450	220	22	20	72	150	8	30	.313 .313 .313 .313	.319 .319 .319 .319	11 11 11 11	.369 .369 .369 .369	.395 .395 .395 .395	20 20 20 20
8.	450	220	22	20	70	160	7	29						

Sample Data Listing for Jet Sew Device

DATA SET 3:  
55/45  
POLYESTER/COTTON

	Heat Temp (F)	Cavity Temp (F)	Heat Time (s)	Pressure (psi)	Cool Temp (F)	Cavity Temp (F)	Cool Time (s)	Cycle Time (s)	dm1	D1	W1	dm2	D2	W2
1.	450	210	20	20	72	160	12	32	.264	.268	10°	.228	.232	10°
2.	450	220	31	20	73	160	16	47	.250	.250	2°	.250	.250	2°
3.	450	220	29	20	71	170	14	43	.264	.263	5	.254	.235	5
4.	450	230	35	20	74	150	26	61	.258	.259	2	.241	.240	2
5.	450	240	51	20	73	150	26	77	.253	.253	0	.241	.232	2



! cotton/polyester

11

[illegible]

#### LIST OF REFERENCES

1. Solinger, Jacob. Apparel Manufacturing Handbook, Second Edition; Bobbin Media Corp., Columbia, South Carolina. 1988.
2. Carnahan, Luther, and Wilkes. Applied Numerical Methods; John Wiley & Sons, New York. 1969.
3. "Equivalence of One- and Two-Phase Models for Heat Transfer Processes in Packed Beds: One-Dimensional Theory"; Vortmeyer and Schaefer, Chemical Engineering Science, 1974, vol. 29, pp. 485-491.
4. Incropera and DeWitt, Fundamentals of Heat and Mass Transfer, Third Edition; John Wiley & Sons, New York. 1990.
5. Theory and Design for Mechanical Measurements; Figliola and Beasley, John Wiley & Sons: 1991.